

Workshop

MRT Methodologies for Real-Time Particle Transport Simulation of Nuclear Systems

Prof. Alireza Haghghat

Virginia Tech

Nuclear Science and Engineering Lab (NSEL)

Nuclear Engineering Program, Mechanical Engineering Department

Arlington, VA, USA

Schedule

- **Part I :** Particle transport & VT MRT methodologies
 - INSPCT-s
 - AIMS
 - TITAN-IR
 - RAPID

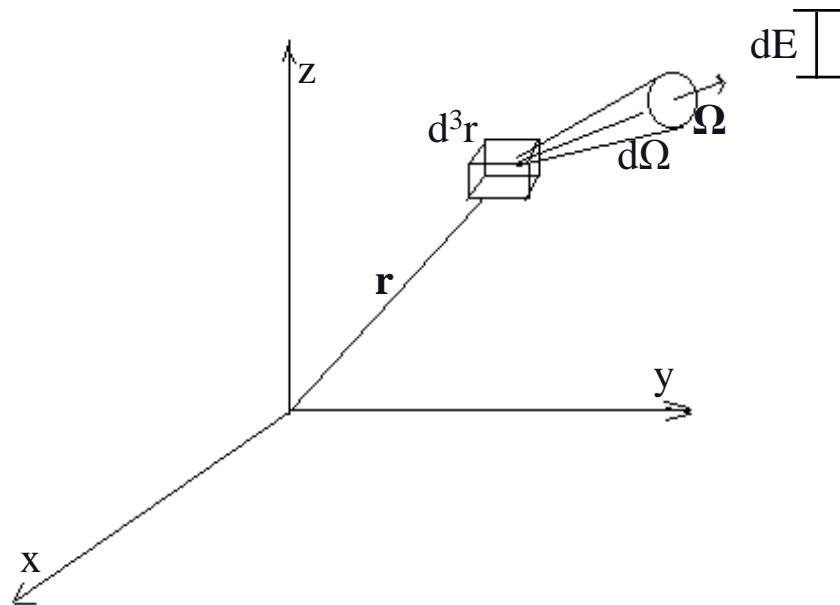
- **Part II:** Demonstrations
 - RAPID
 - INSPCT-s

Particle Transport Theory

Objective

Determine the expected number of particles in a phase space $(d^3rdEd\Omega)$ at time t :

$$n(\vec{r}, E, \hat{\Omega}, t)d^3rdEd\Omega$$



Number density is used to determine angular flux/current, scalar flux and current density, partial currents, and reaction rates.

Simulation Approaches

- **Deterministic Methods**

- Solve the linear Boltzmann equation to obtain the expected flux in a phase space

- **Statistical Monte Carlo Methods**

- Perform particle transport experiments using random numbers (RN's) on a computer to estimate average properties of a particle in phase space

Deterministic – Linear Boltzmann Equation

- **Integro-differential form**

$$\begin{aligned}
 & \text{streaming} \quad \hat{\Omega} \cdot \nabla \Psi(\vec{r}, E, \hat{\Omega}) + \sigma(\vec{r}, E) \Psi(\vec{r}, E, \hat{\Omega}) = \\
 & \quad \quad \quad \text{collision} \\
 & \int_0^{\infty} dE' \int_{4\pi} d\Omega' \sigma_s(\vec{r}, E' \rightarrow E, \hat{\Omega}' \rightarrow \hat{\Omega}) \Psi(\vec{r}, E', \hat{\Omega}') + \\
 & \quad \quad \quad \text{scattering} \\
 & \frac{\chi(E)}{4\pi} \int_0^{\infty} dE' \int_{4\pi} d\Omega' \nu \sigma_f(\vec{r}, E') \Psi(\vec{r}, E', \hat{\Omega}') + S(\vec{r}, E, \hat{\Omega}) \\
 & \quad \quad \quad \text{fission} \quad \quad \quad \text{Independent source}
 \end{aligned}$$

- **Integral form**

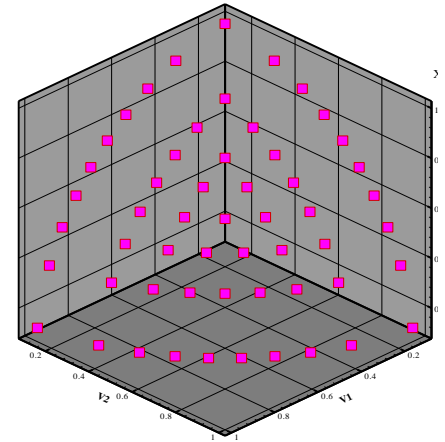
$$\psi(\vec{r}, E, \hat{\Omega}) = \int_0^R d|\vec{r} - \vec{r}'| Q(r') e^{-\tau_E(\vec{r}, \vec{r}')} + \psi(\vec{r}_s, E, \hat{\Omega}) e^{-\tau_E(\vec{r}, \vec{r}_s')}$$

Integro-differential - Solution Method

- **Angular variable: Discrete Ordinates (Sn) method:**

A discrete set of directions $\{ \hat{\Omega}_m \}$
and associated weights $\{ w_m \}$ are selected

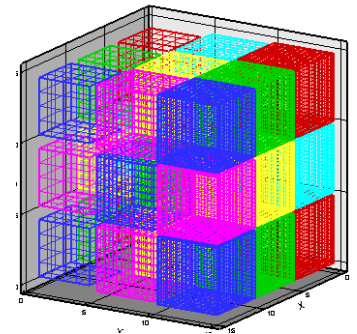
$$\hat{\Omega}_m \cdot \nabla \Psi(\vec{r}, E, \hat{\Omega}_m) + \sigma(\vec{r}, E) \Psi(\vec{r}, E, \hat{\Omega}_m) = q(\vec{r}, E, \hat{\Omega}_m)$$



- **Spatial variable**

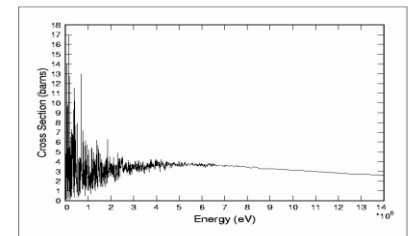
Integrated over fine meshes using FD or FE methods

$$\Psi_{m,g,A} = \frac{\int d^3r \Psi_{m,g}(\vec{r})}{\Delta V_{ijk}}$$



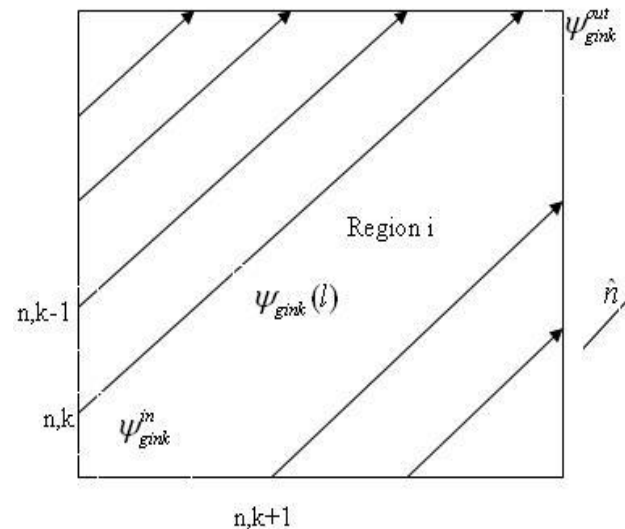
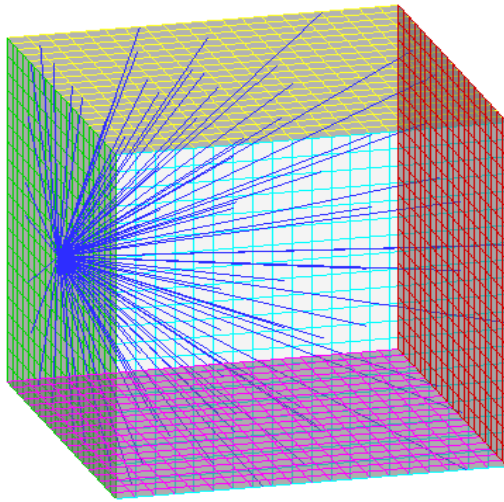
- **Energy variable**

Integrate over energy intervals to prepare multigroup cross sections, σ_g



Integral - Solution method

- **Method of Characteristic (MOC):** Model is partitioned into coarse meshes and transport equation is solved along the characteristic paths (k) (parallel to each discrete ordinate (n)), filling the mesh, and averaged



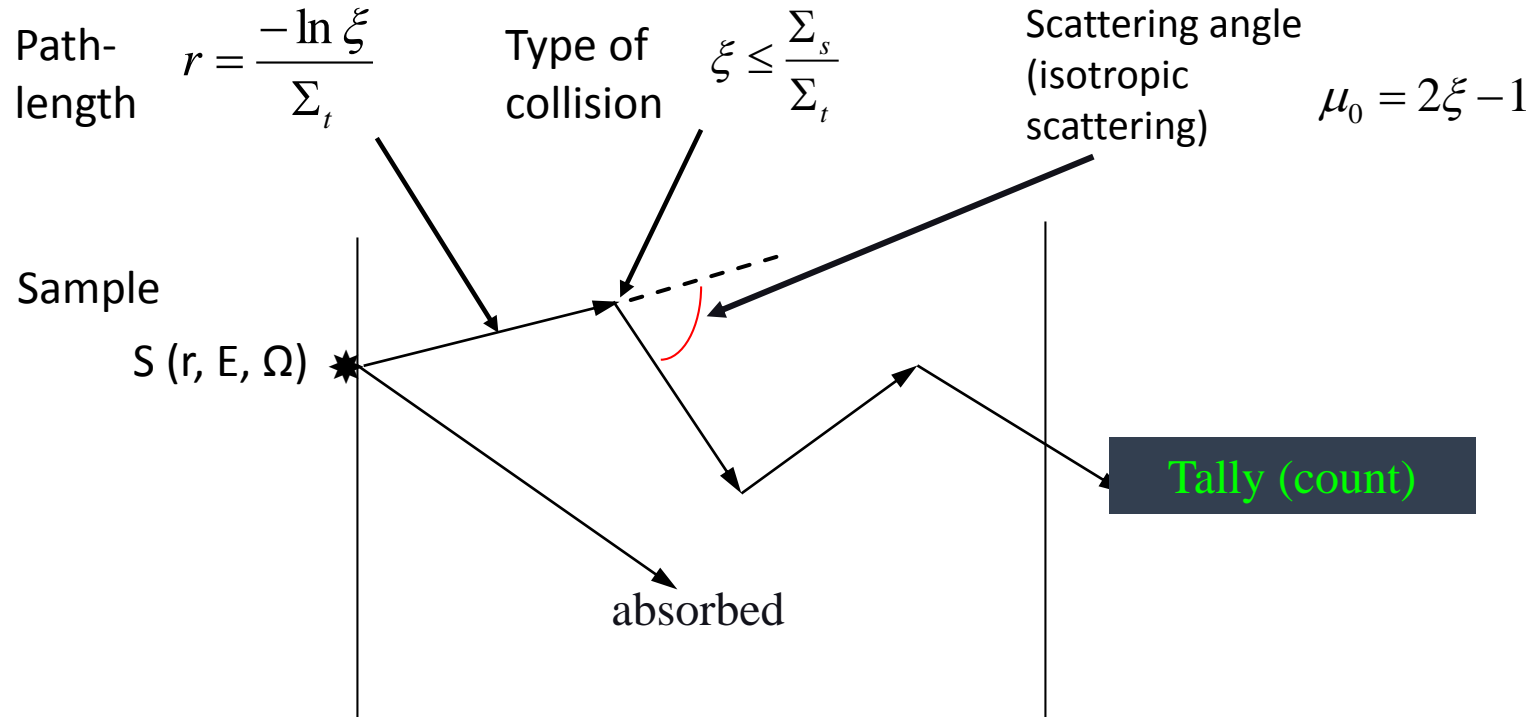
$$\psi_{g,m,i,k}(t_{m,i,k}) = \psi_{g,m,i,k}(0) \exp(-\sigma_{g,i} t_{m,i,k}) + \frac{Q_{g,m,i}}{\sigma_{g,i}} (1 - \exp(-\sigma_{g,i} t_{m,i,k}))$$

Deterministic - Issues/Challenges/Needs

- Robust numerical formulations (e.g., adaptive differencing strategy)
- Algorithms for improving efficiency (i.e., acceleration techniques – synthetic formulations and pre-conditioners)
- Use of advanced computing hardware & software environments
- Pre- and post-processing tools
- Multigroup cross section preparation
- Benchmarking

Monte Carlo Methods

- Perform an experiment on a computer; “exact” simulation of a physical process



Issue:

Precise expected values; i.e., small relative error, $R_{\bar{x}} = \frac{\sigma_{\bar{x}}}{\bar{x}}$

Variance Reduction techniques are needed for real-world problems!

Deterministic vs. Monte Carlo

Item	Deterministic	MC
Geometry	Discrete/ Exact	Exact
Energy treatment – cross section	Discrete	Exact
Direction	Discrete/ Truncated series	Exact
Input preparation	Difficult	simple
Computer memory	Large	Small
Computer time	Small	Large
Numerical issues	Convergence	Statistical uncertainty
Amount of information	Large	Limited
Parallel computing	Complex	Trivial

Approach?

- Why not MC, only?

Because of the difficulty in obtaining **detail information with reliable statistical uncertainty** in a **reasonable time**

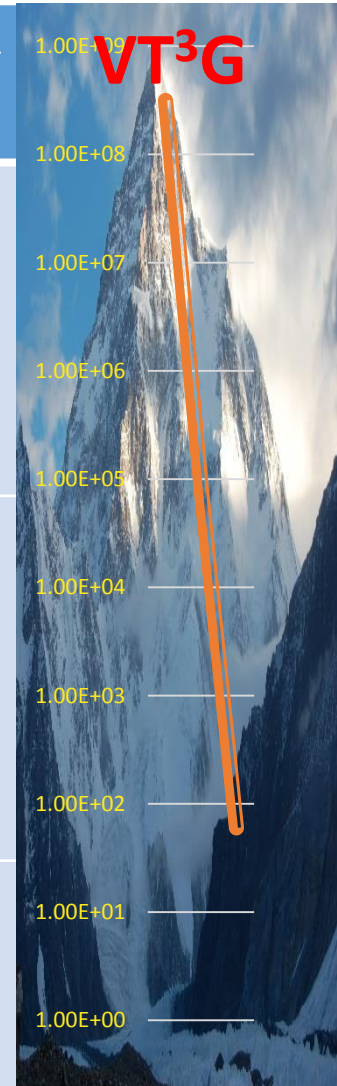
For eigenvalue problems, there are challenges such as **High Dominance Ratio (HDR), under-sampling, and/or correlation between generations**

- Solutions:

- High performance **parallel** computing
- **Hybrid** methods
- **Multi-stage, Response-function Transport (MRT)** methodologies

VT Transport Theory Group VT³G : 30-year Journey

Year	Methodology	Computer code	Wall-clock time
2016	MRT	RAPID	Minutes & Seconds
2015	MRT	TITAN-IR	
2013	MRT	AIMS	
2009	MRT	INSPCTs	
2007	Hybrid MC-det. (AVR)	ADIES (e^-)	Days & Hours
2005	Hybrid det. – det.	TITAN (n, γ)	
1997	Hybrid MC-det. (automated VR - AVR)	A ³ MCNP (n, γ)	
1996	Parallel (3-D)	PENTRAN (n, γ)	Years & Months
1992	Vector & parallel (2-D)		
1989	Parallel processing (1-D)		
1986	Vector processing (1-D)		



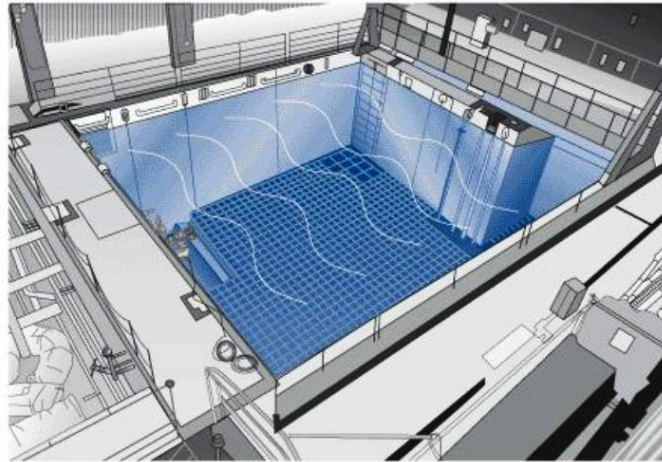
Development of Transport Formulations for Real-Time Applications

- Even parallel & hybrid transport calculations are **slow!**
- The RAPID code system is developed based on the *MRT (Multi-stage Response-function Transport) methodology*; the MRT methodology is described as follows:
 1. *Partition a problem into stages*
 2. *Represent each stage by a response function or set of response coefficients*
 3. *Pre-calculate response functions and/or coefficients (one time)*
 4. *Couple stages through a set of linear system of equations*
 5. *Solve the linear system of equations iteratively in real-time*

MRT Algorithms & Code System

- **2009-Nuclear safeguards: INSPCT-s (Inspection of Nuclear Spent fuel-Pool Calculation Tool ver. Spreadsheet)** for monitoring spent fuel pools for detection of fuel diversion (funded by LLNL)
- **2013 - Nuclear nonproliferation: AIMS (Active Interrogation for Monitoring Special-nuclear-materials)** for monitoring cargo containers (funded by NNSA, in collaboration with Georgia Tech)
- **2015 - Medical image reconstruction: TITAN-IR™ (TITAN with Image Reconstruction)** for deterministic image reconstruction for the SPECT (single photon emission computed tomography) (internal funding, filed for patent)
- **2016 - Nuclear safety, security and nonproliferation: RAPID™ (Real-time Analysis spent fuel Pool *In situ* Detection)** for determination of eigenvalue, subcritical multiplication, pin-wise fission density with axial distribution, and material identification (partly funded DOE, I²S project, led by GaTech) (Ongoing) (filing for patent)

INSPCT-s (funded by LLNL)



Objective – Identification of missing/moved assemblies for safeguards

Approach – On-line combination (via statistical minimization) of measured and computed detector responses to identify possible fuel diversion.

Need?

- A fast and accurate computation tool that in **real time** can estimate the **detector response** for various combinations of
 - Burnup
 - Cooling time
 - Pool lattice arrangement
 - Fuel type (enrichment)

How do we calculate the detector response?

- Standard or “forward” transport, i.e., LBE

$$R = \langle \sigma_d \psi \rangle = \int_{V_d} dV \int_0^\infty dE \int_{4\pi} d\Omega \sigma_d(\vec{r}, E) \psi(\vec{r}, E, \hat{\Omega})$$

where angular flux is obtained using LBE

$$H\psi = S$$

- “Adjoint” (“importance”) function methodology

$$R = \langle S \psi^* \rangle$$

where “importance” function is obtained using the “importance” equation

$$H^* \psi^* = S^*$$

Development of INSPCT-S tool – A MRT algorithm

$$R_n = \langle S_n \phi_n^* \rangle$$

Source ($S = S_{\text{intrinsic}} + S_{\text{subcritical-Multiplication}}$)

Stage 1. Intrinsic Source

- Spontaneous fission & (α, n) from fuel burnup calculation (ORIGEN-ARP)

(Created a database)

Stage 2. Subcritical Multiplication

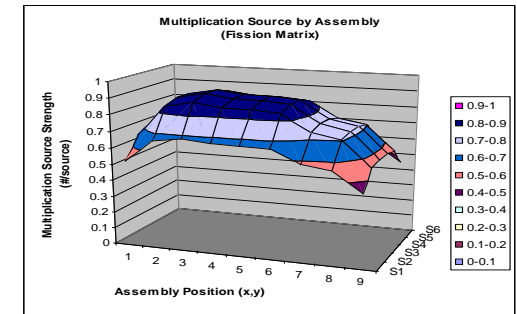
- Fission-Matrix (FM) method**
 - Use MCNP Monte Carlo to obtain $a_{i,j}$ for each pool type

(Created a database for coef. a_{ij})

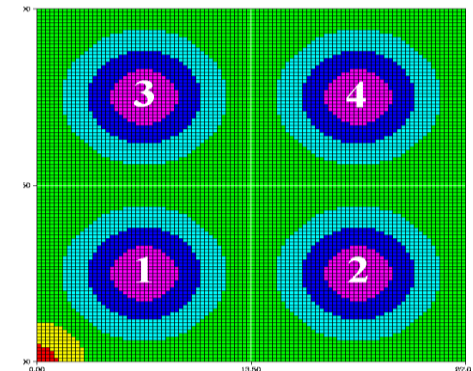
Importance function

Stage 3 – Determine importance function using the deterministic parallel PENTRAN Sn transport code

(Created a database for multigroup adjoint for different lattice sizes)



$$F_i = \sum_{j=1}^N a_{i,j} (F_j + S_j^{\text{int.}})$$



PENTRAN Code System

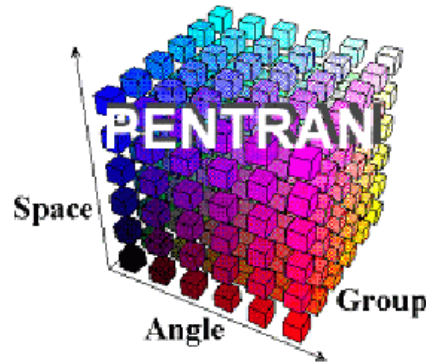
(G. Sjoden and A. Haghghat, 1996)

Pre-processing

PENMSH-XP (prepares mesh, source, and material distributions)

CEPXS (from SNL, prepares multi-groups Cross-section libraries)

S_N Transport
Calculation



(Parallel Environment Neutral-particle TRANsport)

Post-processing

PENPRL (determination of flux via linear interpolation, its comparison with experimental data)

Fission Matrix (FM) Method

- **Eigenvalue** formulation

$$F_i = \frac{1}{k} \sum_{j=1}^N a_{i,j} F_j$$

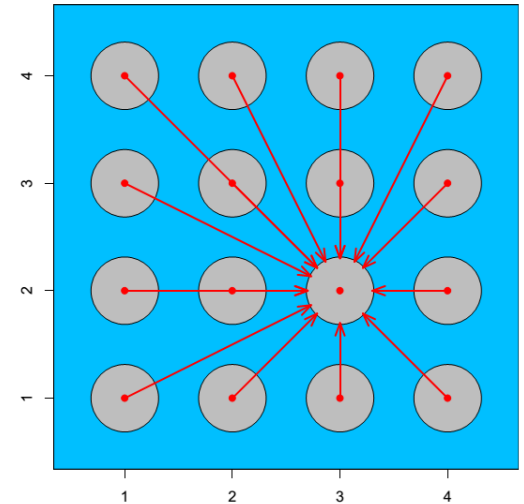
- Where, a is a coefficient matrix, F is fission density, and k is eigenvalue

- **Subcritical multiplication** formulation

$$F_i = \sum_{j=1}^N (a_{i,j} F_j + b_{i,j} S_j),$$

- We have shown that for this application, we can consider

$$a_{i,j} \cong b_{i,j}$$



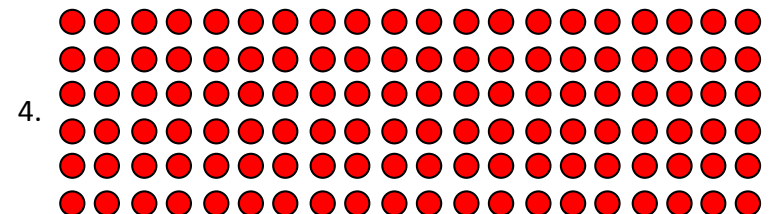
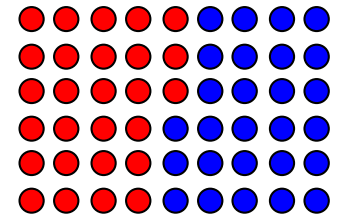
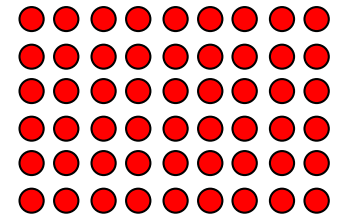
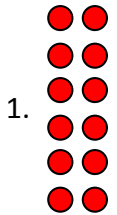
Testing the FM Methodology in INSPCT-s

- Same $a_{i,j}$ coefficients used for every case
- Solve system of equations

$$F_i = \sum_{j=1}^N a_{i,j} (F_j + S_j^{\text{int.}})$$

- Four test spent fuel scenarios

1. 2x6 array, uniform source
2. 9x6 array, uniform source
3. 9x6 array, 27 assemblies on the left with source strength 1, the rest with source strength 0.5
4. 20x6 array, uniform source



- MCNP calculation as a benchmark

FM Results

- Excellent agreement with Monte Carlo (<1%)

Assembly Arrangement Case	M (MCNP)	M (Fission Matrix)	Difference	MCNP Uncertainty 1-σ
2x6, uniform	1.7133	1.7104	-0. 29%	0.0008
9x6, uniform	1.9988	1.9966	-0. 22%	0.0007
9x6, non-uniform	2.0033	1.9968	-0.65%	0.0013
20x6, uniform	2.0513	2.0444	-0. 69%	0.0012

- Very fast
<1s for Fission-matrix method as compared to ~1hr for the standard Monte Carlo

Real-time Tool: INSPCT-s (Inspection of Nuclear Spent fuel-Pool Computing Tool –Spreadsheet)

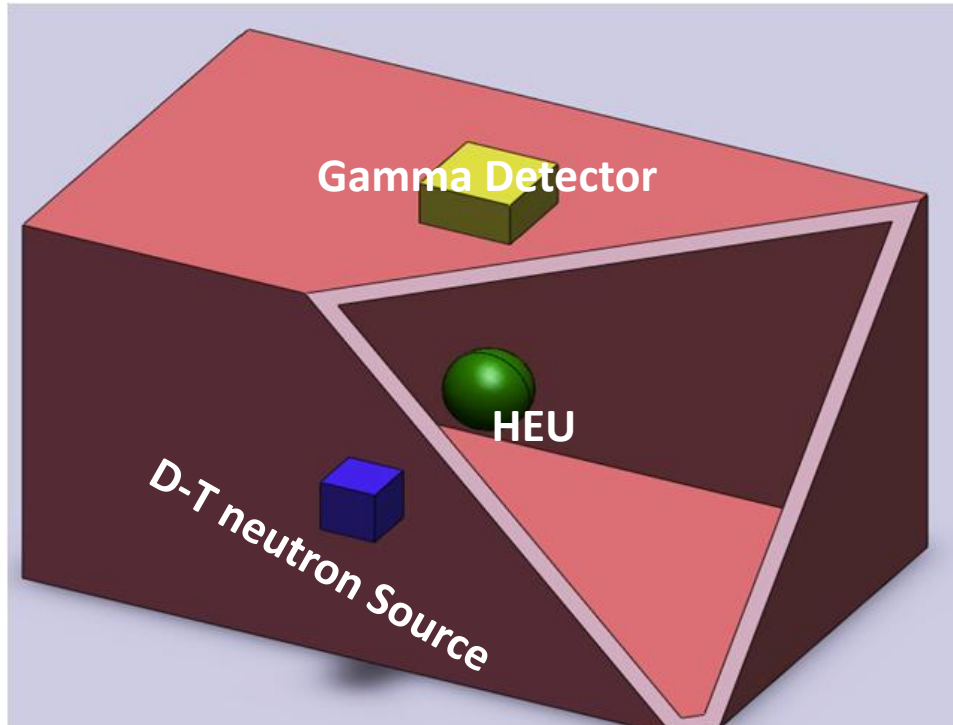
INSPCT-S solves $R_n \equiv \langle S_n \phi^* \rangle$ (Use of Fission Matrix & importance function)

By interpolating the database, source and importance function are determined

INPUT										OUTPUT											
		src file		C:\Users\ali\Documents\haghD\uftg\LLNL\INSPCT-s\se.dsrc								Detector Normalization									
COLUMNS		8 fm file		C:\Users\ali\Documents\haghD\uftg\LLNL\INSPCT-s\se						Response Tolerance		5.28E-10									
ROWS		6 imp file		C:\Users\ali\Documents\haghD\uftg\LLNL\INSPCT-s\se						15.00%											
		Burnup										Independent Source									
(x,y)	1	2	3	4	5	6	7	8	(x,y)	1	2	3	4	5	6	7	8				
1	9000	9000	9000	9000	9000	9000	9000	9000	1	4.60E+07	3.39E+07	2.84E+07	2.48E+07	2.21E+07	1.94E+07	1.56E+07	13036948				
2	10000	10000	10000	10000	10000	10000	10000	10000	2	6.89E+07	5.30E+07	4.49E+07	3.86E+07	3.39E+07	2.91E+07	2.26E+07	18101692				
3	11000	11000	11000	11000	11000	11000	11000	11000	3	1.00E+08	8.04E+07	6.86E+07	5.84E+07	5.06E+07	4.29E+07	3.23E+07	25047256				
4	12000	12000	12000	12000	12000	12000	12000	12000	4	1.42E+08	1.17E+08	1.01E+08	8.51E+07	7.33E+07	6.15E+07	4.53E+07	34204842				
5	13000	13000	13000	13000	13000	13000	13000	13000	5	1.98E+08	1.67E+08	1.45E+08	1.22E+08	1.04E+08	8.67E+07	6.28E+07	46492994				
6	14000	14000	14000	14000	14000	14000	14000	14000	6	2.68E+08	2.32E+08	2.01E+08	1.69E+08	1.44E+08	1.19E+08	8.52E+07	62072007				
		Cooling time										Fission Source									
(x,y)	1	2	3	4	5	6	7	8	(x,y)	1	2	3	4	5	6	7	8				
1	1	2	5	10	15	20	30	40	1	4.03E+07	4.68E+07	4.25E+07	3.66E+07	3.11E+07	2.57E+07	1.98E+07	12521188				
2	1	2	5	10	15	20	30	40	2	6.88E+07	8.12E+07	7.41E+07	6.34E+07	5.32E+07	4.33E+07	3.26E+07	20199639				
3	1	2	5	10	15	20	30	40	3	9.82E+07	1.17E+08	1.07E+08	9.08E+07	7.54E+07	6.05E+07	4.47E+07	27169878				
4	1	2	5	10	15	20	30	40	4	1.32E+08	1.58E+08	1.44E+08	1.21E+08	9.98E+07	7.93E+07	5.78E+07	34751134				
5	1	2	5	10	15	20	30	40	5	1.62E+08	1.92E+08	1.73E+08	1.45E+08	1.19E+08	9.42E+07	6.80E+07	40823941				
6	1	2	5	10	15	20	30	40	6	1.49E+08	1.74E+08	1.56E+08	1.30E+08	1.06E+08	8.38E+07	6.03E+07	36229288				
		Response (experimental)										Response(Calculated)									
(x,y)	0.5	1.5	2.5	3.5	4.5	5.5	6.5	7.5	8.5	(x,y)	0.5	1.5	2.5	3.5	4.5	5.5	6.5	7.5	8.5		
0.5										0.5	0.123198	0.230998	0.221266	0.193583	0.166627	0.141523	0.114534	0.083892	-0.036614		
1.5		0.6				0.3				1.5	0.305453	0.580498	0.561644	0.491674	0.420538	0.353999	0.28285	0.203871	0.087599		
2.5			0.8							2.5	0.467647	0.897903	0.880437	0.770597	0.653747	0.543993	0.427576	0.301569	0.127819		
3.5				1.4						3.5	0.658686	1.271323	1.252983	1.094413	0.922518	0.761393	0.591298	0.410909	0.172554		
4.5					1.2					4.5	0.879337	1.696988	1.669344	1.453015	1.219392	1.002015	0.772365	0.532245	0.222616		
5.5										5.5	1.029258	1.978009	1.923356	1.665877	1.394836	1.14574	0.880125	0.605581	0.253192		
6.5										6.5	0.57336	1.093457	1.058167	0.914234	0.765146	0.628852	0.482792	0.332139	0.139652		
		Response Difference										Response Difference									
(x,y)	0.5	1.5	2.5	3.5	4.5	5.5	6.5	7.5	8.5	(x,y)	0.5	1.5	2.5	3.5	4.5	5.5	6.5	7.5	8.5		
0.5										0.5											
1.5										1.5		3.36%				-15.25%					
2.5										2.5			3.82%								
3.5										3.5				3.65%							
4.5										4.5					4.74%						
5.5										5.5											
6.5										6.5											



Active Interrogation for Monitoring Special-nuclear-materials (AIMS)



Identified 4 stages

Stage 1 - Neutron transport & subcritical multiplication (VT)

Stage 2 - Fission neutron and gamma transport and generation of gamma source (VT)

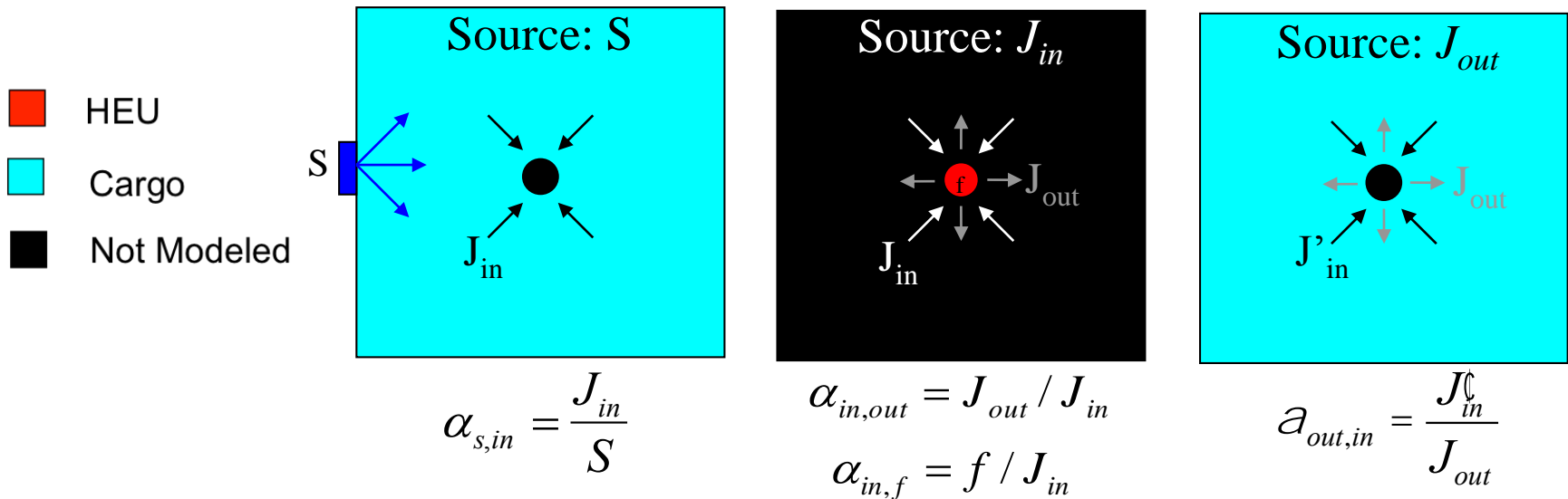
Stage 3 - Transport of gamma-ray to the detector; current/angular gamma flux (VT)

Stage 4 - Detector response (GaTech)

Cargo Container	243.84 x 259.08 x 283.456 cm ³
Cargo material	Hydrogenous material, e.g., Third-density water
Neutron source	D-T (14.1 MeV), 13.5 x 13.5 cm ²
SNM	25 kg sphere of HEU, radius = 6.75 cm
Detector window	13.5 x 13.5 cm ²

Stage 1: Calculation of fission neutron density due to subcritical multiplication

- A response function methodology is developed for:
 - neutron transport within the cargo container
 - subcritical multiplication (fission neutron source density)
- The model is split into: **cargo and region-of-interest (ROI)**, and a sequence of fixed-source problems are solved using MCNP5



- Then, the fission rate F is given by

$$F = S a_{s,in} \left(a_{in,f} + \frac{a_{in,f} a_{in,out} a_{out,in}}{1 - a_{in,out} a_{out,in}} \right)$$

Stage 2: Transport of fission neutron and gamma, and generation of gamma source

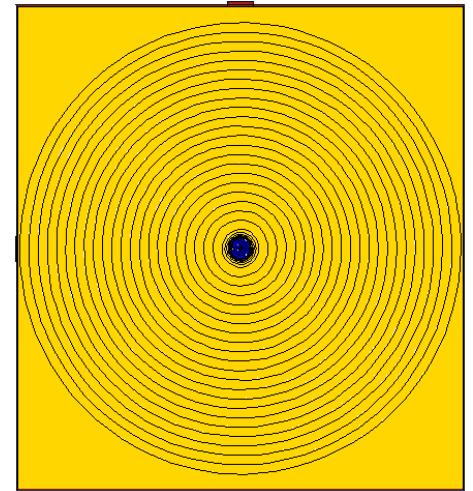
Stage 2.1 – Transport of fission neutron and gamma

- Assume the flux distribution is radially symmetric around the HEU
- MCNP calculation to obtain normalized fission neutron flux as a function of distance

$$\tilde{\phi}_g^n$$

- Flux at any point (x, y, z) can be calculated as

$$f_g^n(x, y, z) = F \tilde{f}_g^n \left(\sqrt{(x - x_0)^2 + (y - y_0)^2 + (z - z_0)^2} \right)$$



Stage 2.2 - Gamma source distribution is obtained by

$$S_{i,g}^\gamma = \sum_{g'} \phi_{i,g'}^n \sigma(n, \gamma)_{i,g' \rightarrow g}$$

Stage 3: Determine gamma current at detector window

An adjoint methodology is used to determine the gamma current at the detector window due to fission neutrons

forward transport equation, $H\psi = S,$

$$\text{where } H = \hat{W} \cdot \nabla + S(\vec{r}, E) - \int_0^\infty dE' \int_{4\pi} dW' S_s(\vec{r}, E' \rightarrow E, \hat{W}' \cdot \hat{W})$$

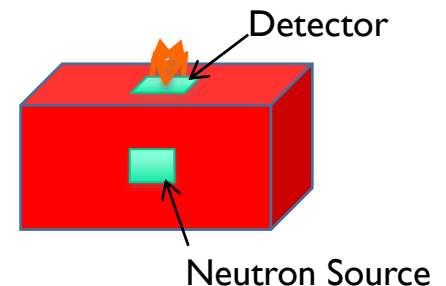
adjoint transport equation, $H^\dagger \psi^\dagger = S^\dagger,$

$$\text{where } H^\dagger = -\hat{W} \cdot \nabla + S(\vec{r}, E) - \int_0^\infty dE' \int_{4\pi} dW' S_s(\vec{r}, E \rightarrow E', \hat{W} \cdot \hat{W}')$$

The boundary conditions are given by

$$\psi = 0 \text{ for } \hat{n} \cdot \hat{\Omega} < 0 \text{ on } \Gamma$$

$$\psi^\dagger = d(E - E_g) d(\vec{r} - \vec{r}_d) \text{ for } \hat{n} \cdot \hat{W} > 0 \text{ on } G_d$$



Stage 3 (continued)

Form the commutation relation between the forward & adjoint equations:

$$\langle \mathcal{Y}^\dagger H \mathcal{Y} \rangle - \langle \mathcal{Y} H^\dagger \mathcal{Y}^\dagger \rangle = \langle \mathcal{Y}^\dagger S \rangle - \langle \mathcal{Y} S^\dagger \rangle$$

The adjoint source S^\dagger is defined as zero and only the streaming term on the left-hand side will remain so this equation reduces to

$$\int_0^\infty dE \int_{4\pi} d\Omega \int_V d^3r \nabla \cdot \hat{W} \mathcal{Y}(\vec{r}, E, \hat{W}) \mathcal{Y}^\dagger(\vec{r}, E, \hat{W}) = \langle \mathcal{Y}^\dagger S \rangle$$

Using the divergence theorem and expanding into two integrals over \wedge

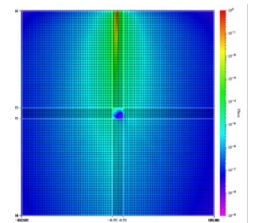
$$\int_0^\infty dE \int_{\hat{n} \cdot \hat{W} > 0} d\Omega \int_G dG \hat{n} \cdot \hat{W} \mathcal{Y} \mathcal{Y}^\dagger + \int_0^\infty dE \int_{\hat{n} \cdot \hat{W} < 0} d\Omega \int_G dG \hat{n} \cdot \hat{W} \mathcal{Y} \mathcal{Y}^\dagger = \langle \mathcal{Y}^\dagger S \rangle$$

Applying the boundary conditions gives

$$\int_0^\infty dE \int_{\hat{n} \cdot \hat{W} > 0} d\Omega \int_G dG (\hat{n} \cdot \hat{W}) \mathcal{Y}(\vec{r}, E, \hat{W}) d(E - E_g) d(\vec{r} - \vec{r}_d) = \langle \mathcal{Y}^\dagger S \rangle$$

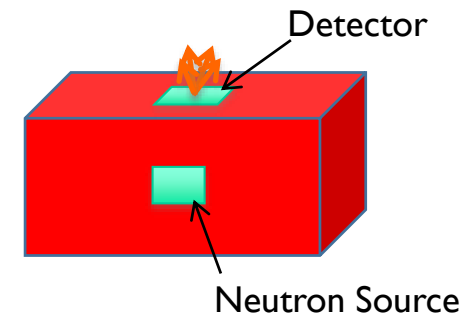
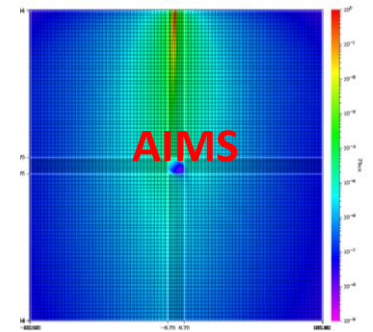
$$J_+(\vec{r}, E_g) = \langle \mathcal{Y}^\dagger S \rangle = \sum_i \sum_{g'} f_{i,g'}^\dagger S_{i,g'} DV_i$$

Where, **Adjoint function** is calculated using the **TITAN 3-D parallel transport code**



Demonstration of AIMS Software

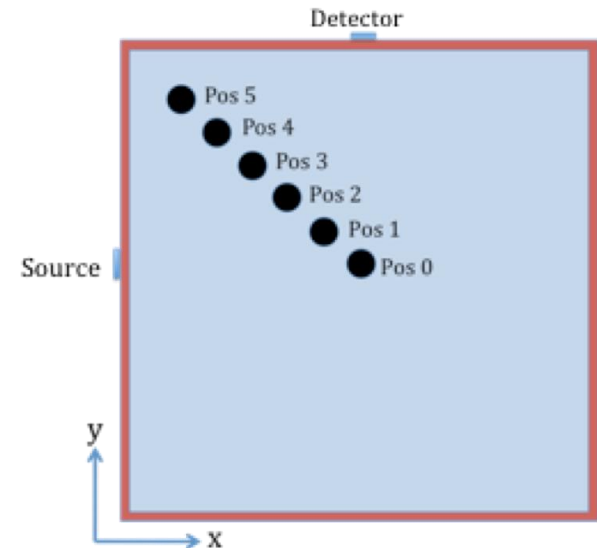
- Developed the Active Interrogation for Monitoring Special-nuclear-materials (AIMS) software tool
- AIMS performs one-time pre-calculation to prepare coefficients and adjoint function distributions for different cargo materials, then calculates gamma current at the detector window in *real time* using steps 1-3.



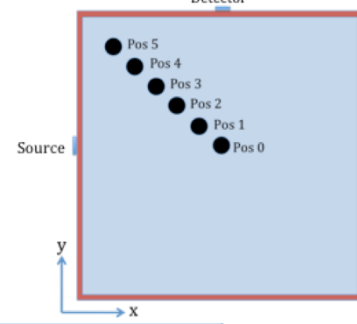
Cases Simulated

- 6 different HEU positions within the cargo container are considered
- For each HEU position, simulate scanning the source-detector assembly along the long axis (z-axis) of the container started from the center
- All cases used the same coefficients (**HEU at center; not in adjoint model**)
- Compares the AIMS method calculated current with a reference MCNP5 solution

HEU Position	(x cm, y cm)
0	(0,0)
1	(-20,20)
2	(-40,40)
3	(-60,60)
4	(-80,80)
5	(-100,100)



Results



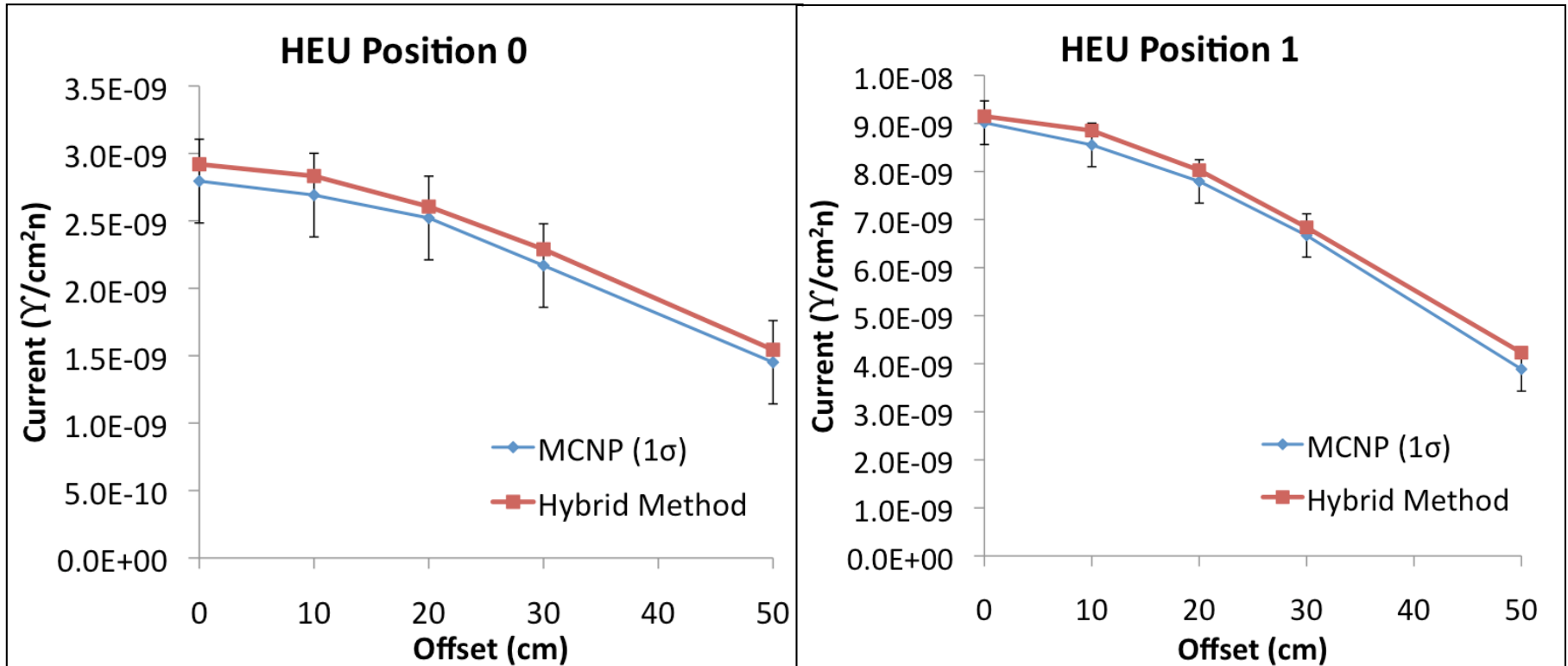
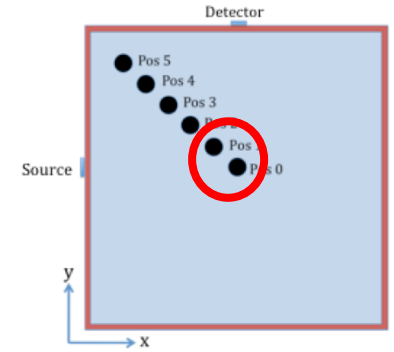
Total fission rate: Response method vs. MCNP5

ROI Position	Fission Rate		
	MCNP (1σ)	AIMS	Difference (%)
0*	5.55E-03 (0.09%)	5.60E-03	1.01%
1*	1.07E-02 (0.09%)	1.03E-02	-1.88%
2*	1.72E-02 (0.15%)	1.66E-02	-3.16%
3*	2.00E-02 (0.14%)	1.99E-02	-0.74%
4 ⁺ position specific coef.	-	1.57E-02	1.81%
5 ⁺ position specific coef.	-	7.05E-03	-1.85%

*Response coefficients were calculated for an HEU sphere located at the container center.

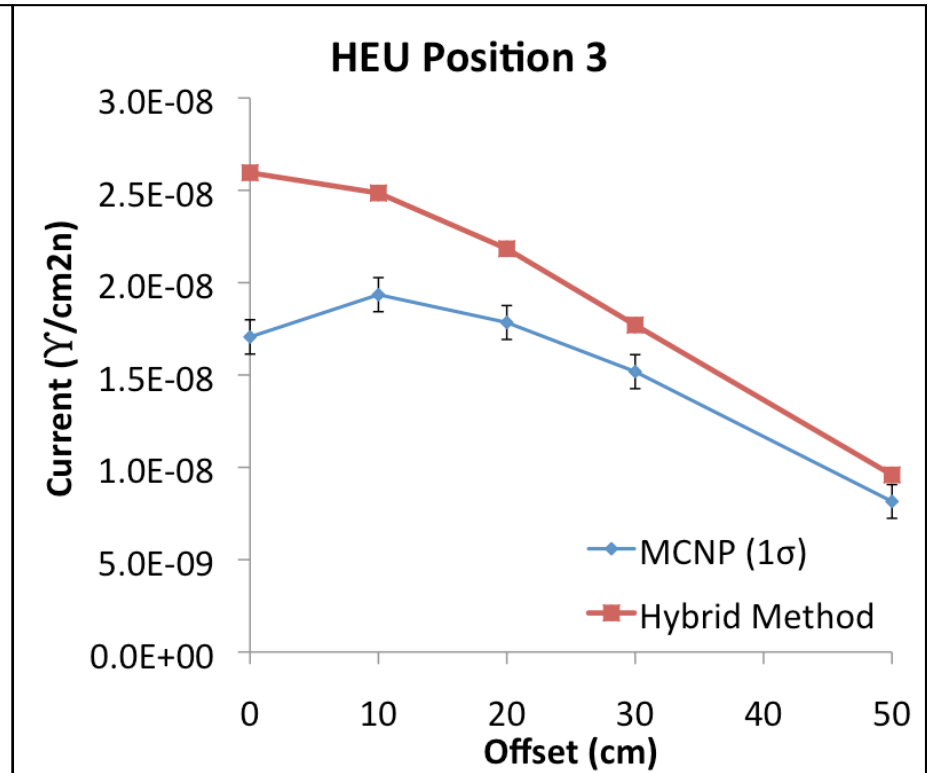
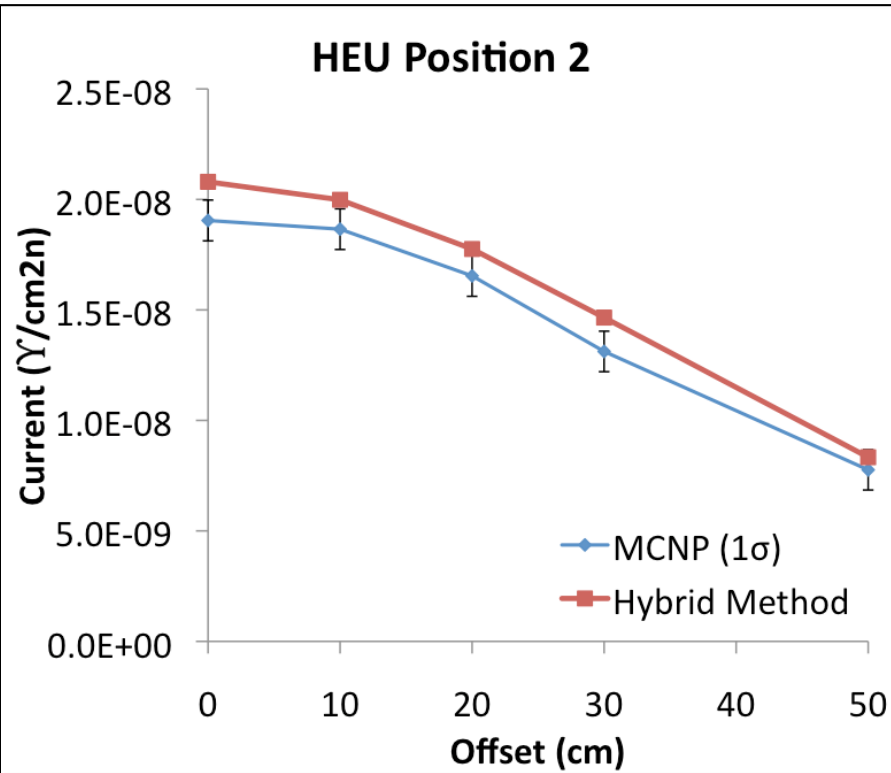
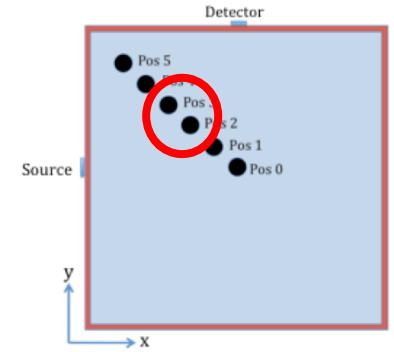
+ Response coefficients were calculated for an HEU sphere located at its actual position.

Comparison Gamma Currents, AIMS vs. MCNP



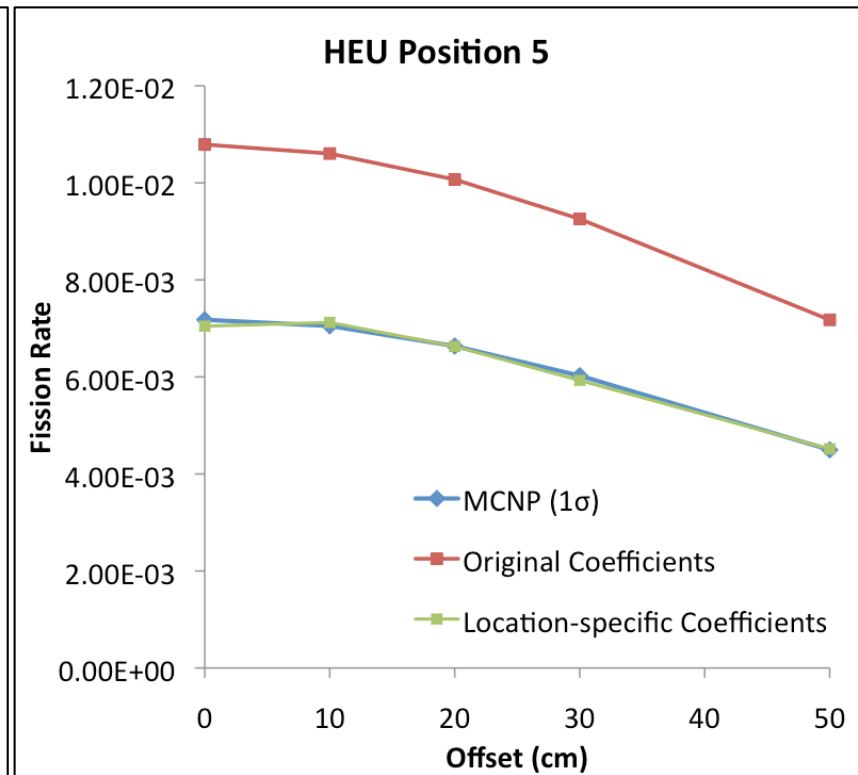
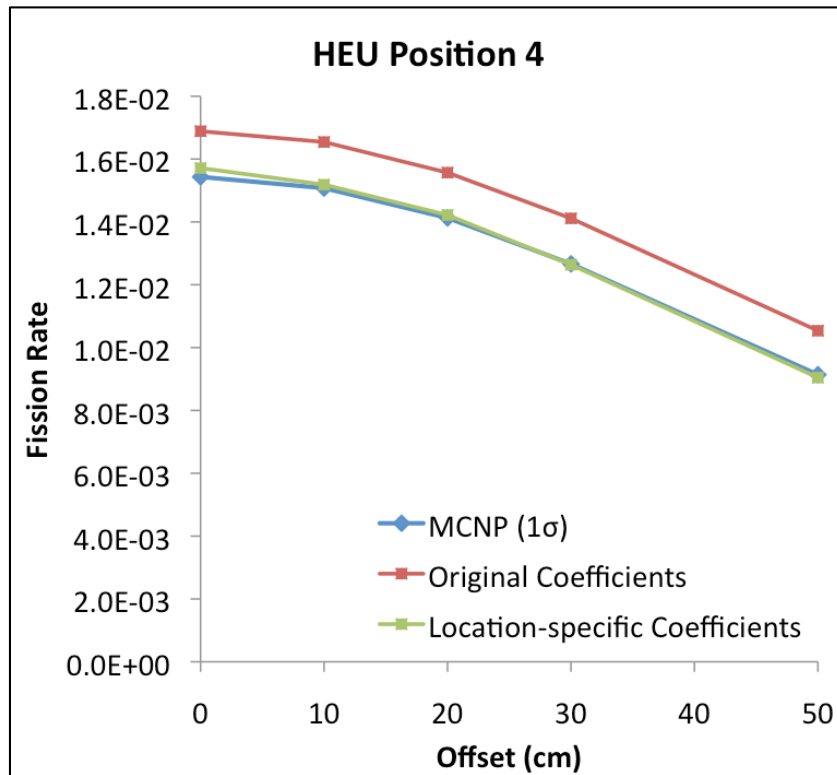
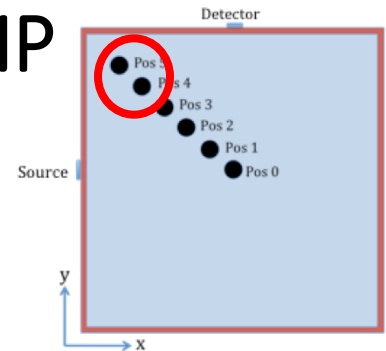
Note: Adjoint function determine without presence of HEU

Comparison of Gamma Currents, AIMS vs. MCNP



Comparison Fission Rate, AIMS vs. MCNP

- $\alpha_{s,in}$ recalculated for the actual positions



*MCNP error bars smaller than data points (~0.1%)

Computing Time

Pre-calculated Database Computation Times

Response coefficients (serial)	60 hours
Group 8 adjoint function (8 cores)	5.9 hours

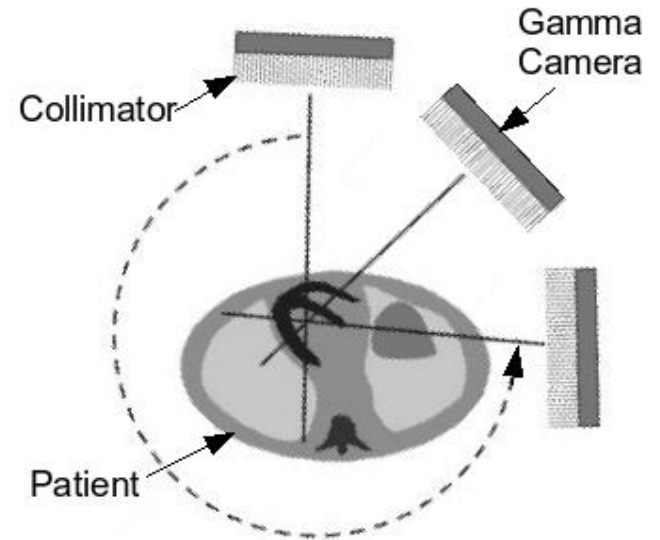
Computation Time for 5 Scanning Locations

AIMS for all HEU positions (1 core)		0.06 hours (3.6 min)
MCNP5* (8 cores)	HEU position 0 or 5	495 hours (20.7 days)
	HEU position 1	254 hours (10.6 days)
	HEU position 2, 3, or 4	63 hours (2.6 days)

*Times are for the MCNP5 uncertainties given in plots (4.8%-32.3%), i.e., some of the results are NOT reliable

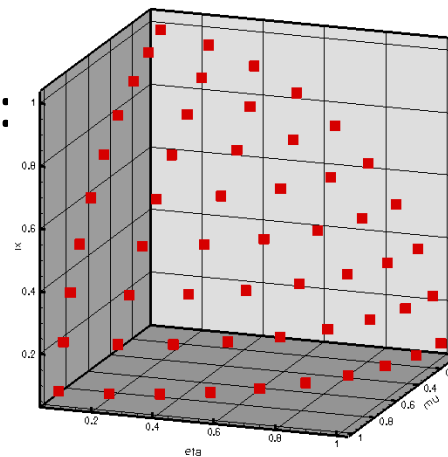
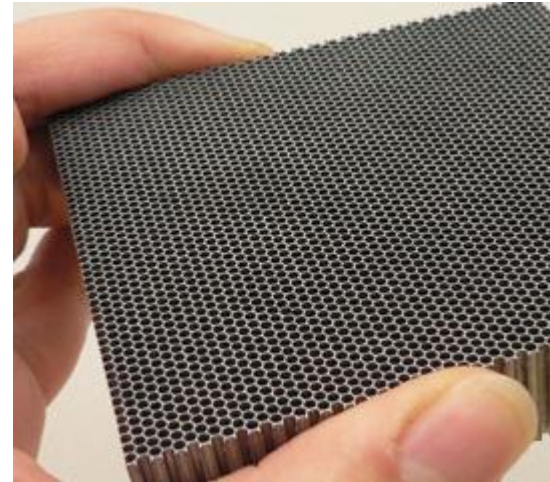
Introduction to Single Photon Emission Computed Tomography (SPECT)

- 17 million procedures in the US in 2010
- Nuclear medicine imaging procedure used to examine myocardial perfusion, bone metabolism, thyroid function, etc.
- *Functional* imaging modality
- Radiopharmaceutical injected/ingested and localizes in a part of the body
- Emitted radiation detected at a gamma camera to form 2D projection images at different angles
- Collimator in front of the gamma camera provides spatial resolution
- Projection images can be reconstructed to form a 3D image of the radionuclide distribution

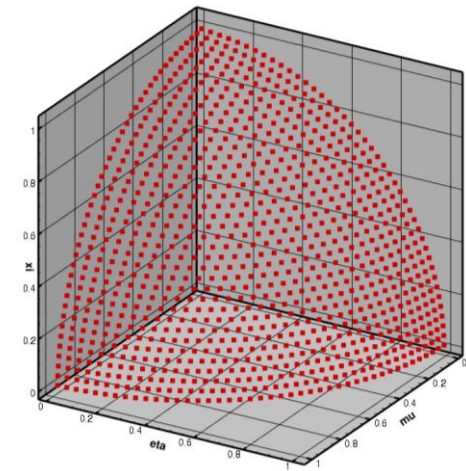


TITAN Deterministic SPECT Simulation

- The collimator in SPECT poses a challenge for deterministic modeling:
 - Spatial discretization
 - Angular discretization
- Typical dimensions include:
 - Hole diameter ~ 0.18 cm
 - Septa thickness ~ 0.02 cm
 - Length ~ 3.3 cm
 - Acceptance Angle $\sim 1.6^\circ$



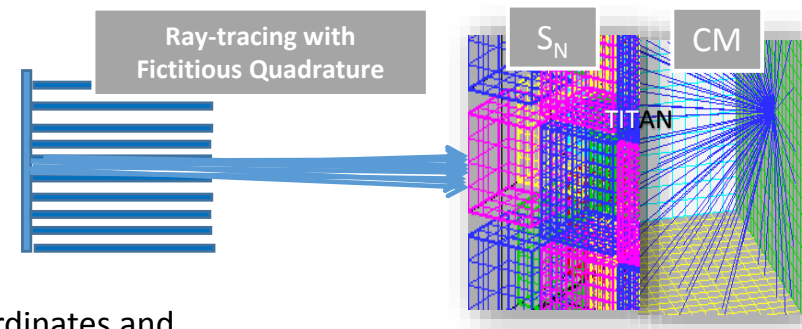
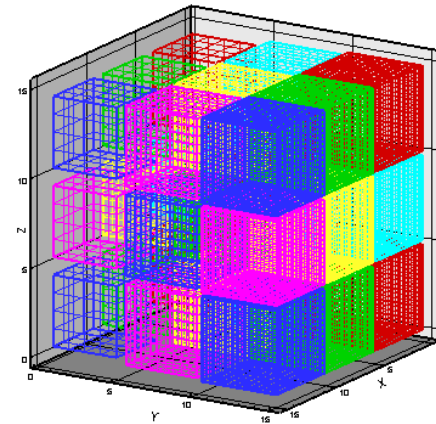
S_{20} Quadrature Set
(440 directions)



S_{86} Quadrature Set
(7568 directions)

Determination of the *importance function* (ψ^*)

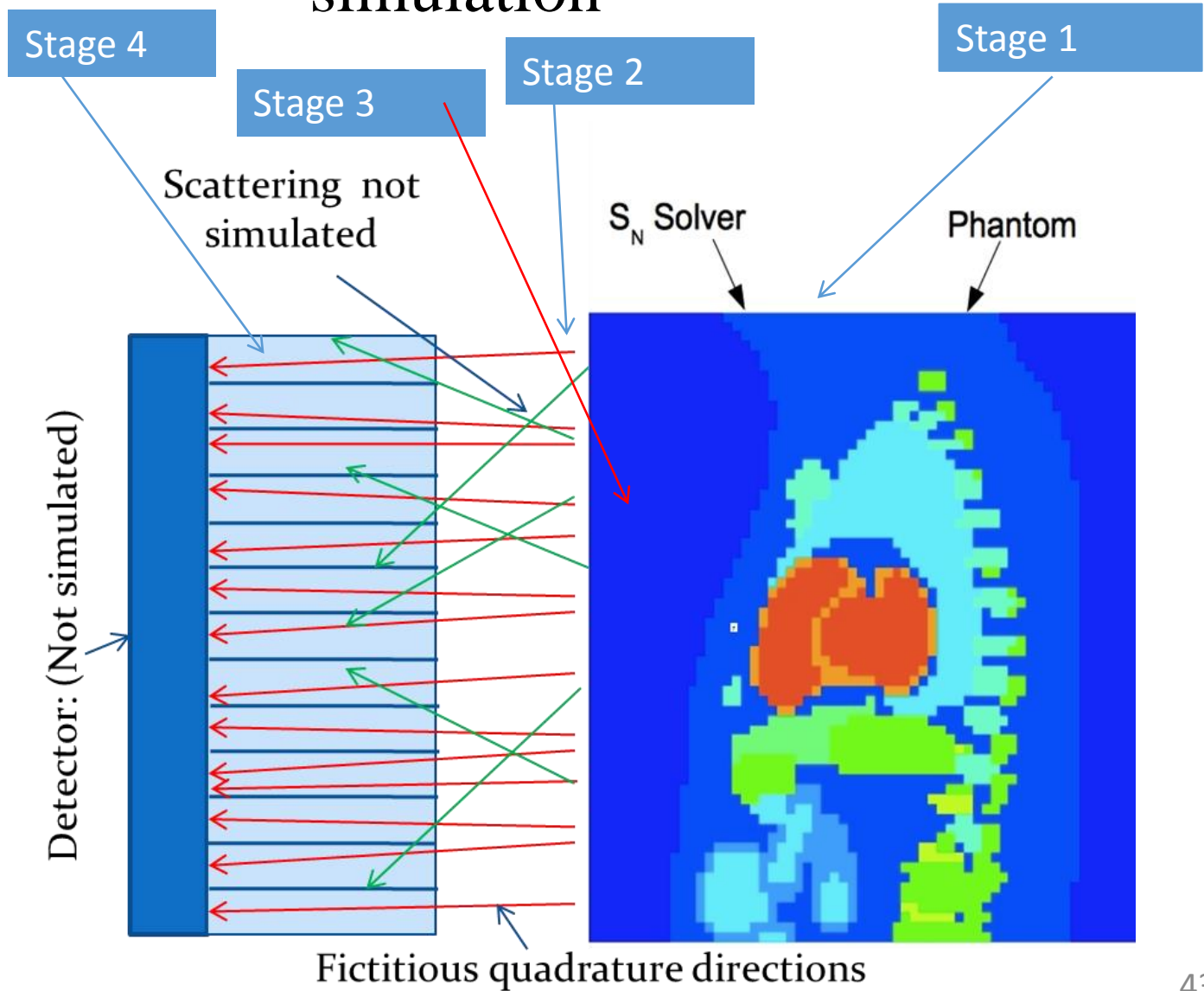
- The TITAN *multigroup, parallel hybrid transport code system*
- TITAN was developed by Yi and Haghghat in 2006. It is a hybrid deterministic code by partitioning the problem domain into coarse meshes and allowing the use of different transport solvers within each coarse mesh.
- TITAN is written in F90 with some features from F2003 (object oriented23), and uses MPI for parallel processing
- The current version of TITAN allows for the following solvers:
 - 1) Discrete Ordinates (S_N) Solver
 - 2) Characteristics Method (CM) Solver
 - 3) Simplified ray-tracing with fictitious quadrature set



*C. Yi and A. Haghghat, "A 3-D Block-Oriented Hybrid Discrete Ordinates and Characteristics Method," *Nuclear Science and Engineering*, **164**, pp. 221-247 (2010).

4-Stage TITAN Hybrid formulation for SPECT simulation

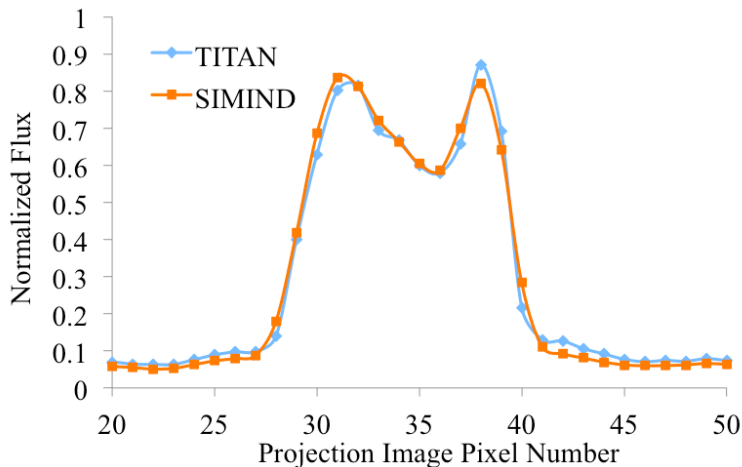
- Stage 1- S_n calculation in phantom
- Stage 2 – Selection of fictitious angular quadrature & Circular OS (COS) directions
- Stage 3 – S_n with fictitious quadrature
- Stage 4 – ray tracing



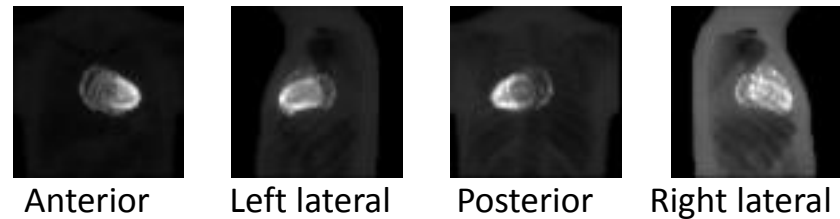
Example of Benchmarking TITAN Projection Images

SIMIND Comparison

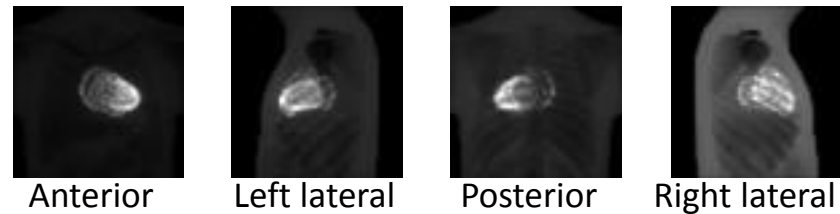
NURBS-based cardiac-torso (NCAT) phantom with Tc-99m (140 keV)



SIMIND generated projection images



TITAN generated projection images



Number of Projection Images	1	4	8	45	90
SIMIND Time (sec)	17	67	140	754	1508
TITAN Time (sec)	200	202	212	274	352

Times are for a single processor

Image Reconstruction

- Filtered backprojection (FBP) (Cormack 1963)
 - Analytic image reconstruction
 - Traditional standard for reconstruction due to speed and simplicity
 - Issues: filter choice, amplification of high-freq. noise, streak artifacts, cannot incorporate system details
- Algebraic reconstruction technique (ART) (Gordon *et al.* 1970)
 - Iterative constraint-based reconstruction
 - Allows the incorporation of prior knowledge
 - Issues: noisy, computationally expensive
- Maximum likelihood expectation maximization (ML-EM) (Shepp & Vardi 1982)
 - Iterative statistical reconstruction
 - For emission tomography, has recently surpassed FBP in popularity
 - Advantages include: Poisson statistics, nonnegativity constraint, incorporation of system details
 - Issues: increasing noise, computationally expensive

ML-EM Brief Derivation

Mean number of photons detected in detector bin d :

$$\bar{n}_d = \sum_{b=1}^B p_{b,d} \hat{l}_b$$

$p_{b,d}$: probability that photon emitted in voxel b is detected in bin d (system matrix)
 \hat{l}_b : mean number of emissions in voxel b

Number of detected particles is a Poisson random variable, so the probability of detecting n_d^* photons in detector bin d :

$$P(n_d^*) = e^{-\bar{n}_d} \frac{\bar{n}_d^{n_d^*}}{n_d^*!}$$

Likelihood function:

$$L(\hat{l}) = P(n_d^* | \hat{l}) = \prod_{d=1}^D P(n_d^*) = \prod_{d=1}^D \frac{e^{-\bar{n}_d} \bar{n}_d^{n_d^*}}{n_d^*!}$$

Log-likelihood will have the same maximum location:

$$\begin{aligned} \ln(L(\hat{l})) &= \sum_{d=1}^D \left(-\bar{n}_d + n_d^* \ln(\bar{n}_d) - \ln(n_d^*) \right) \\ &= \sum_{d=1}^D \hat{e} - \sum_{b=1}^B p_{b,d} \hat{l}_b + n_d^* \ln \left(\sum_{b=1}^B p_{b,d} \hat{l}_b \right) - \ln(n_d^*) \end{aligned}$$

Take derivative and set to zero to find maximum:

$$\frac{\partial \ln(L(\hat{l}))}{\partial \hat{l}_d} = -\sum_{d=1}^D p_{b,d} + \sum_{d=1}^D \frac{n_d^*}{\sum_{b'=1}^B p_{b',d} \hat{l}_{b'}} p_{b,d} = 0$$

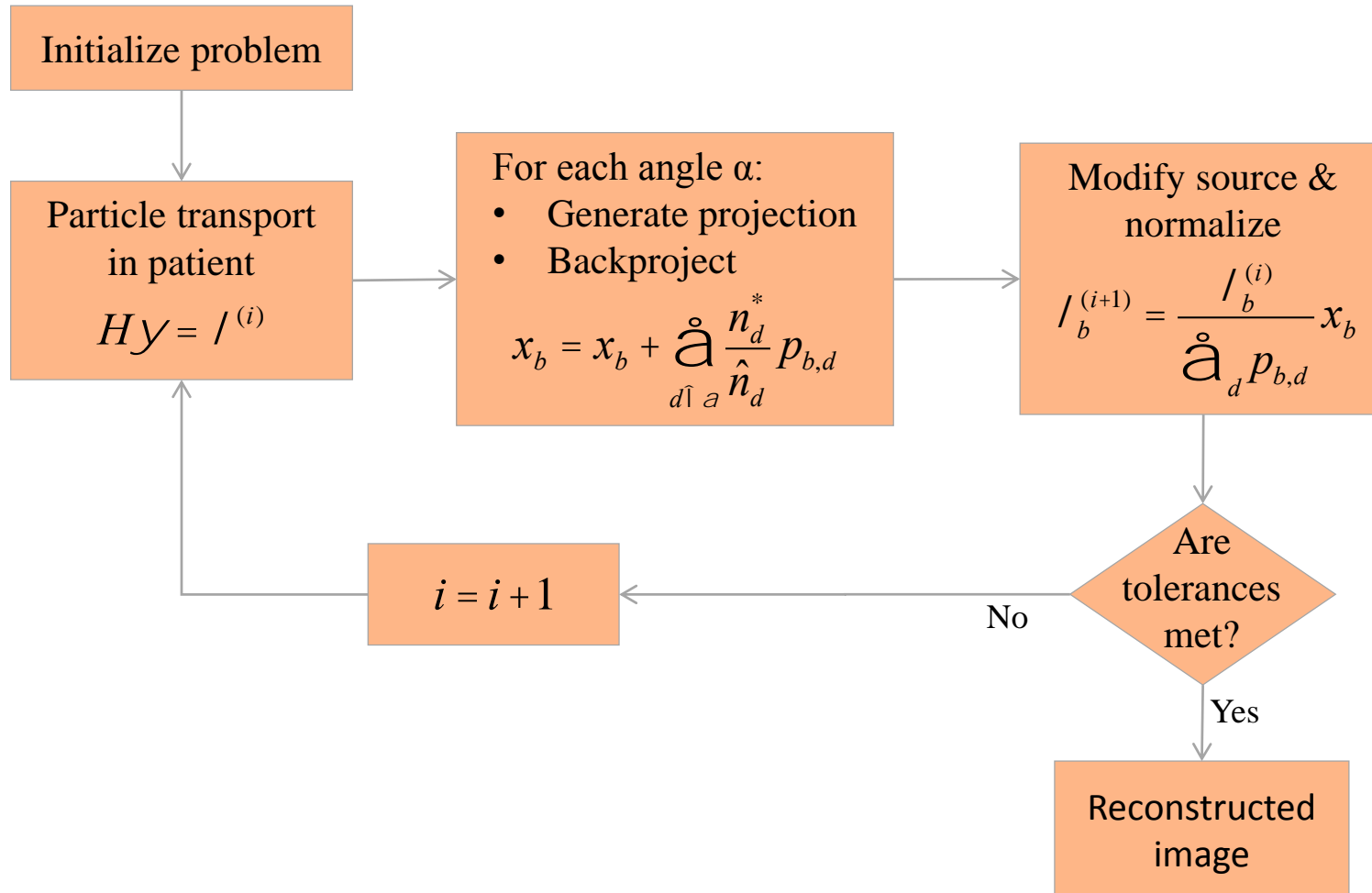
Multiply by \hat{l}_b and solve:

$$\hat{l}_b^{(i+1)} = \frac{\hat{l}_b^{(i)}}{\sum_{d=1}^D p_{b,d}} \sum_{d=1}^D \frac{n_d^*}{\sum_{b'=1}^B p_{b',d} \hat{l}_{b'}^{(i)}} p_{b,d}, \quad b = 1, \dots, B$$

ML-EM can be viewed as a series of projections and backprojections

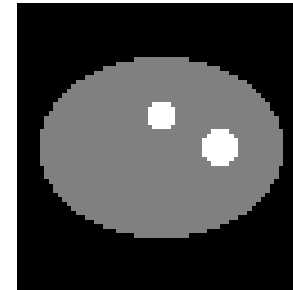
$$\text{Source}^{(i+1)} = \text{Source}^{(i)} \cdot \text{Backprojection of } \frac{\text{Measured Projections}}{\text{Estimated Projections}}$$

TITAN with Image Reconstruction (TITAN-IR)

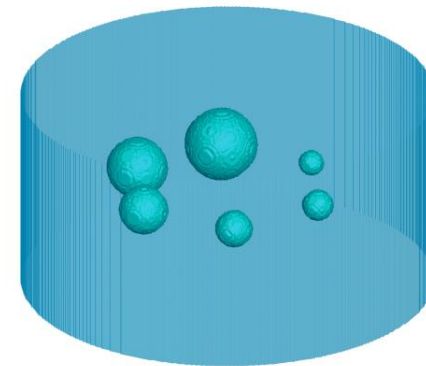


Analyzing TITAN-IR

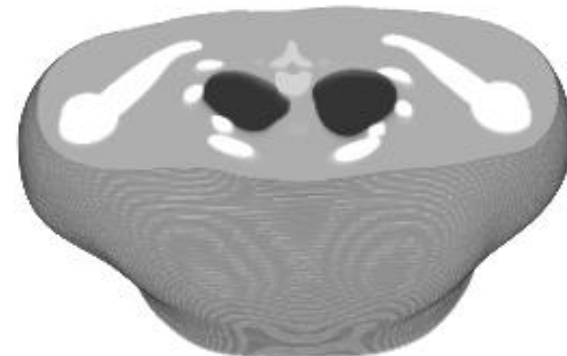
1) 2-D elliptical water phantom with two circles of high intensity source (i.e., lesions)



2) **Jaszczak: 3-D quality assurance phantom, cold sphere region**



3) NCAT: NURBS-based cardiac-torso, 3-D heterogeneous phantom



Reconstruction Analysis

- Visually display reconstructed images
- Plot profiles through important areas of reconstructed images
- Quality metrics:

- Mean relative error (MRE)

$$\text{MRE} = \frac{1}{N_d} \sum_{d=1}^{N_d} \frac{|\hat{n}_d^{(i)} - n_d^*|}{n_d^*}$$

- Mean squared error (MSE)

$$\text{MSE} = \frac{1}{N_d} \sum_{d=1}^{N_d} (\hat{n}_d^{(i)} - n_d^*)^2$$

$\hat{n}_d^{(i)}$ = counts in detector bin d at iteration i

n_d^* = measured counts in detector bin d

- Contrast

$$C_l = \frac{\bar{I}_l - \bar{I}_0}{\bar{I}_0}$$

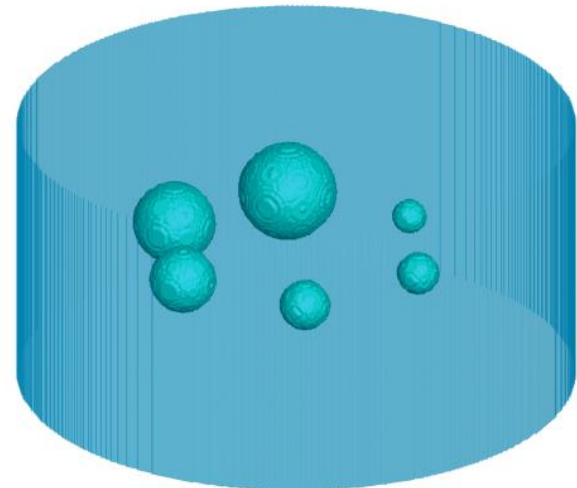
- Noise = $\frac{1}{\bar{I}_0} \sqrt{\frac{\sum_{i=1}^{N_V} (I_i - \bar{I}_0)^2}{N_V - 1}}$

\bar{I}_l = average source intensity in lesion

\bar{I}_0 = average reference background intensity

2) Jaszczak Cold Sphere Phantom

- 6 cold spheres with radii of 0.635, 0.795, 0.955, 1.27, 1.59, and 1.9 cm
- 185 MBq Tc-99m source (140 keV)
- Reference projection data obtained at 64 angles over 360° using SIMIND
- System matrix $p(b,d)$
 - Generated by Image Reconstruction Toolbox in MATLAB (models attenuation but not scatter)
 - Dimensions of (64x64x32) by (64x32x64)
- Initial guess is a uniform source distribution
- Three cases of projection data:
 - 1) No noise & no collimator blur
 - 2) Noisy & no collimator blur
 - 3) Noisy collimated data



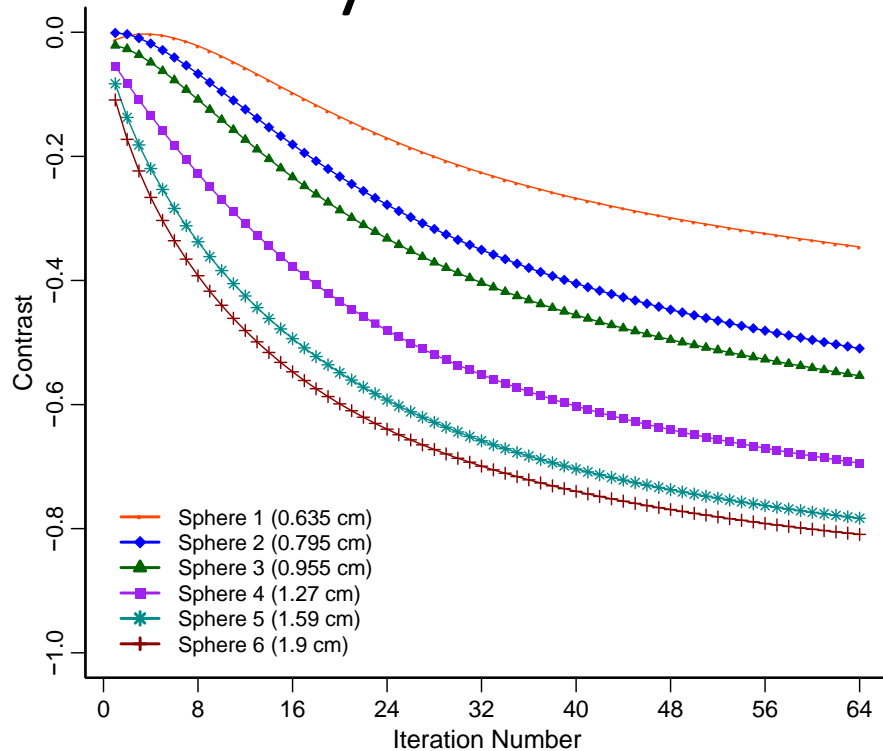
Jaszczak Cold Sphere Phantom: Noisy Collimated Projection Data

Collimator	Hole Diameter	Septa Thickness	Length	Acceptance Angle
GE-LEGP*	0.25 cm	0.03 cm	4.10 cm	1.83°
SE-LEHR†	0.111 cm	0.016 cm	2.405 cm	1.39°

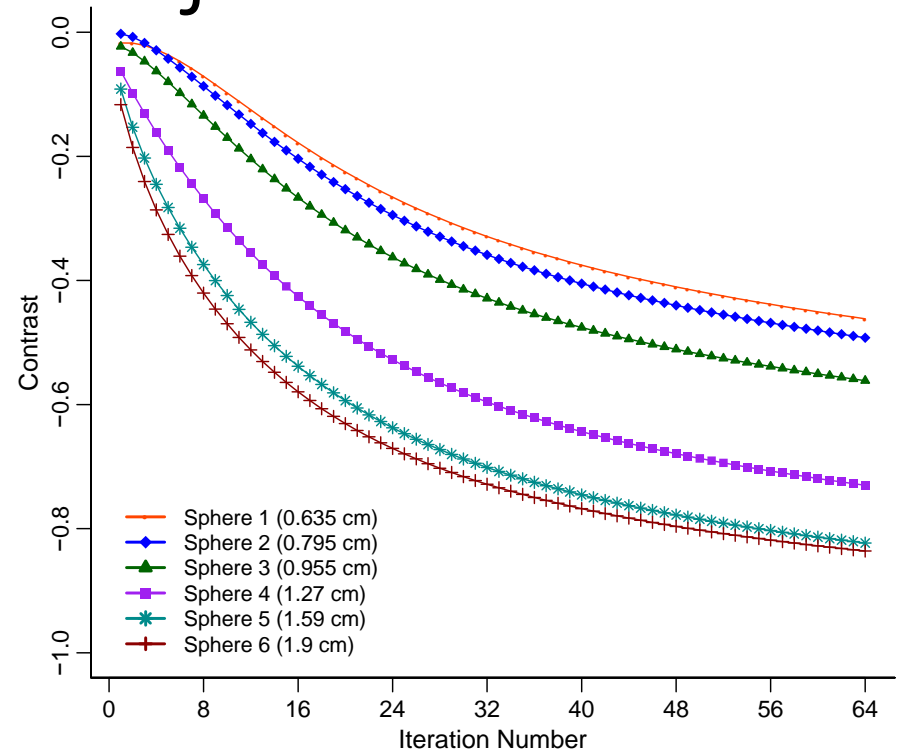
*General Electric – Low energy, general purpose collimator

†Siemens – Low energy, high resolution collimator

Jaszczak Cold Sphere Phantom: Noisy Collimated Projection Data



Contrast in each cold sphere (radius) for
noisy GE-LEGP (1.83°) projection data



Contrast in each cold sphere (radius) for
noisy SE-LEHR (1.39°) projection data

Jaszczak Cold Sphere Phantom: Noisy Collimated Projection Data



Reconstruction of noisy
GE-LEGP data



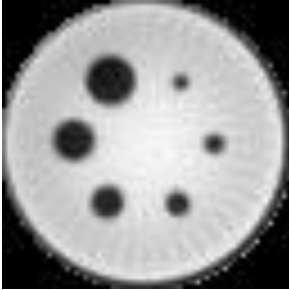
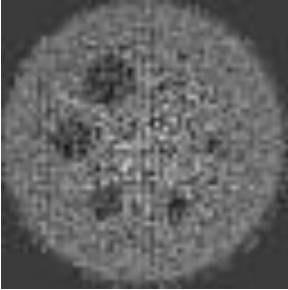
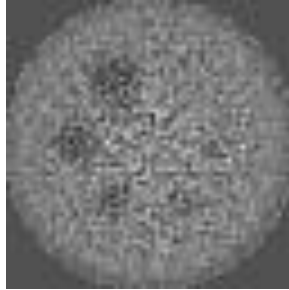
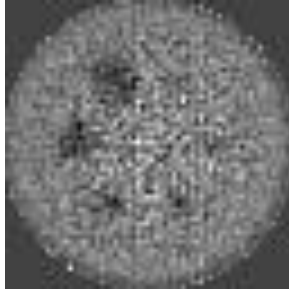

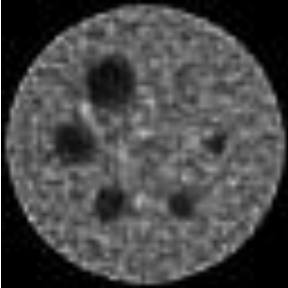
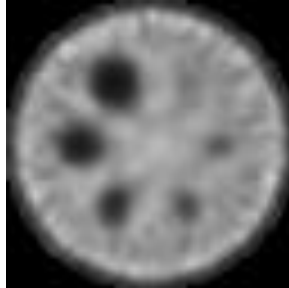
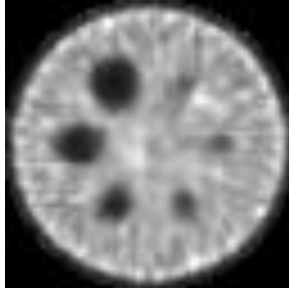
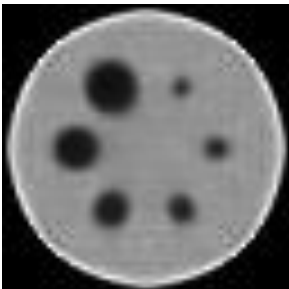
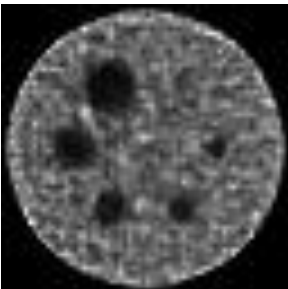
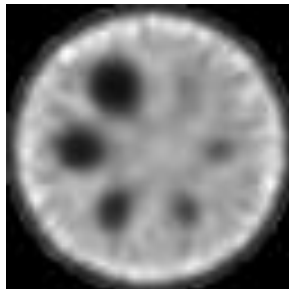
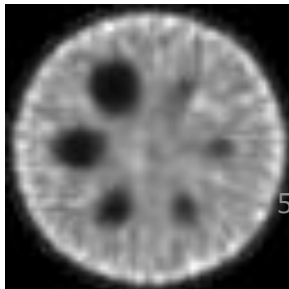
Reconstruction of noisy SE-
LEHR data

Comparison of TITAN-IR with Other Methods Based on Jaszczak Phantom:

- Filtered backprojection (FBP)
 - Traditional standard for image reconstruction
 - Implemented in MATLAB and includes the Chang attenuation correction*
- ML-EM with System Matrix (SM) only
 - Standard ML-EM reconstruction method
 - Algorithm written in Fortran 90
 - Uses the same system matrix that TITAN-IR uses for backprojection

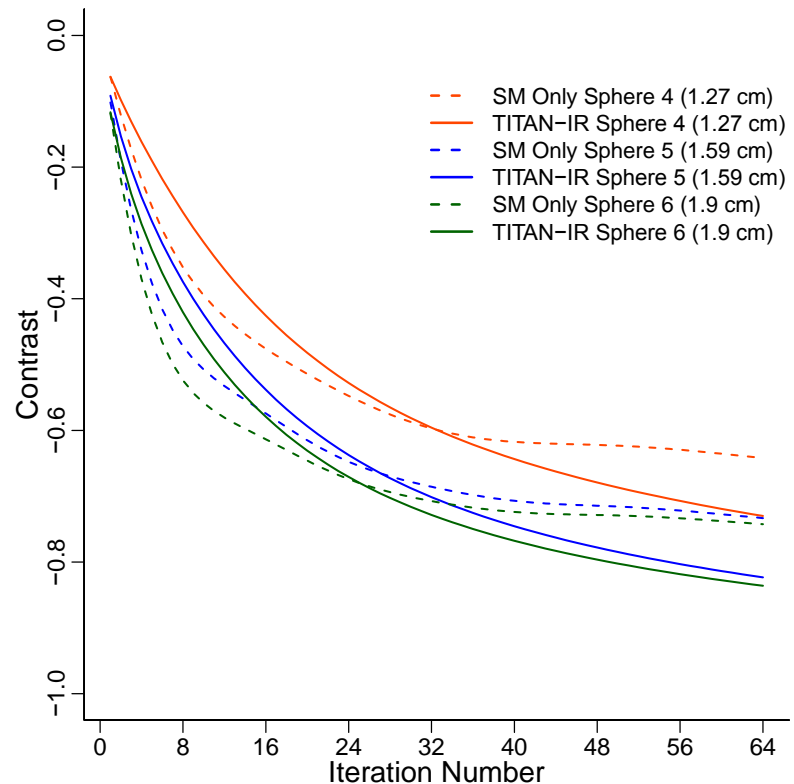
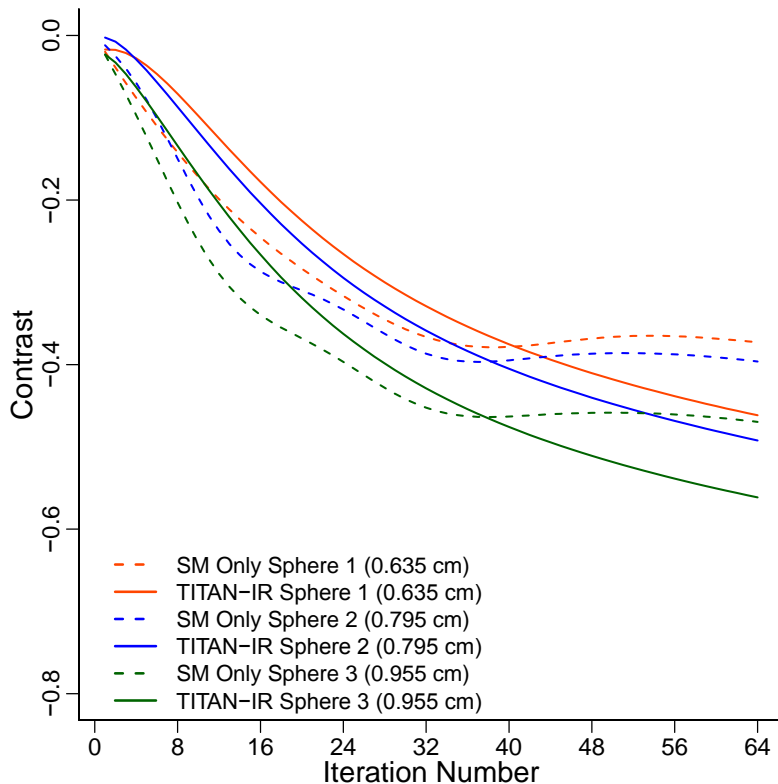
*L.-T.Chang, "A method for attenuation correction in radionuclide computed tomography," *IEEE Trans. Nucl. Sci.*, 1978

Comparison of Methods with Jaszczak Phantom

Algorithm	Noiseless, no collimator blur	Noisy, no collimator blur	Noisy GE-LEGP	Noisy SE-LEHR
FBP				
ML-EM with SM only				
TITAN-IR				

Comparison of Methods with Jaszczak Phantom

- Contrast in reconstruction of noisy SE-LEHR projection data



Computation Time

Jaszczak phantom: Noisy GE-LEGP projection data

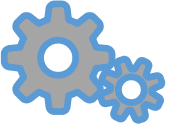
Computing environment [Up to 16 cores, Intel Xeon E5 2.6 GHz processors, 16 GB per core]

Processor Cores	Wall Clock Time (s)	Speedup
1	1665.7	-
2	905.1	1.8
4	524.3	3.2
8	341.4	4.9
16	172.0	9.7

Spent fuel Pool & Cask Modeling

- **Standard approach - Full Monte Carlo calculations face difficulties in this area**
 - Convergence is difficult due to undesampling (due to absorbers)
 - Convergence can also be difficult to detect
 - Computation times are very long, especially to get detailed information
 - Changing pool configuration requires complete recalculation

The RAPID (Real-time Analysis for Particle transport and In-situ Detection) code system



RAPID™ Code System

- RAPID is capable of calculating the system eigenvalue k_{eff} , pin-wise axially-dependent 3D fission density distribution, and detector response.
- RAPID is comprised of **six stages**:

Pre-calculation

Stage 1 – Calculation of material concentration

Stage 2 - Calculation of fission matrix (FM) coefficients

Stage 3 - Calculation of field-of-view (FOV)

Stage 4 – Calculation of importance function

Calculation

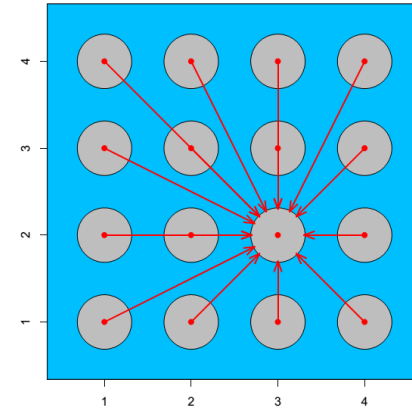
Stage 5 - Processing of FM coefficients & Solution of a linear system of equations (i.e., FM formulation)

Stage 6 – Calculation of Detector response

Determination of fission Matrix (FM) Coefficients

- **Eigenvalue** formulation

$$F_i = \frac{1}{k} \sum_{j=1}^N a_{i,j} F_j$$



- k is eigenvalue
- F_j is fission source, S_j is fixed source in cell j
- $a_{i,j}$ is the number of fission neutrons produced in cell i due to a fission neutron born in cell j .

- **Subcritical multiplication** formulation

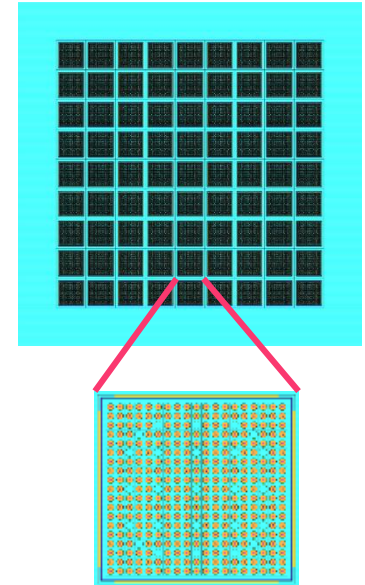
$$F_i = \sum_{j=1}^N (a_{i,j} F_j + b_{i,j} S_j),$$

- $b_{i,j}$ is the number of fission neutrons produced in cell i due to a source neutron born in cell j .

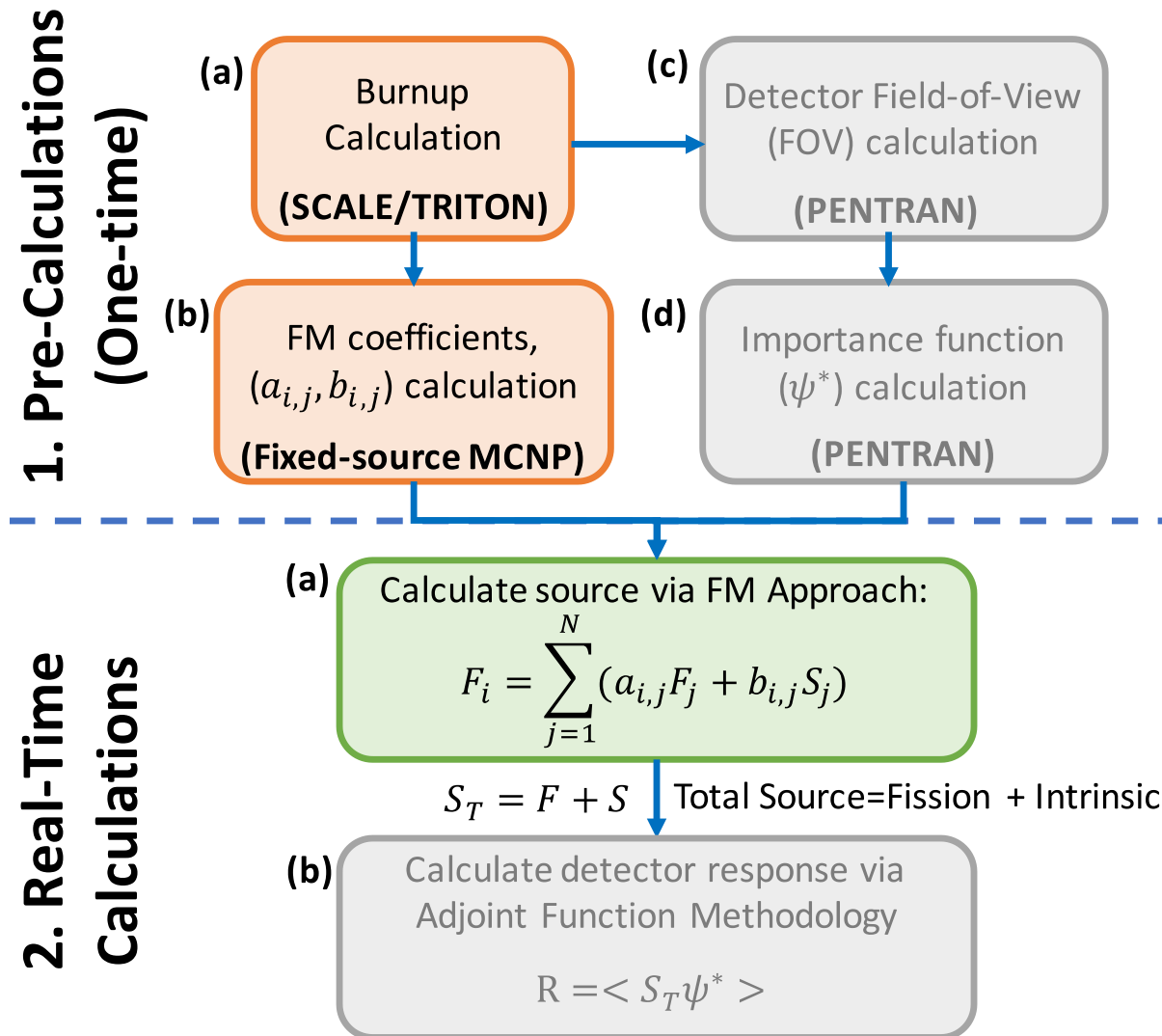
FM Coefficients Determination : a Multi-layer approach

- **Brute force approach:**
 - For a typical spent nuclear fuel pool with a sub-region of 9x9 assemblies:
$$N = 9 \times 9 \times 264 = 21,384 \text{ total fuel pins}$$
 - Considering 24 axial segments per rod, then
$$N = 513,216$$
 - Standard FM would require $N = 513,216$ separate fixed-source calculations to determine the coefficient matrix
 - A matrix of size $N \times N = 2.63391E+11$ total coefficients (> 2 TB of memory is needed)
- The straightforward approach is clearly **NOT feasible**
- **Multi-layer, regional approach** (*in the process of filing for a patent*)
 - Determine coefficients as a function of different parameters (**Stage 1**)
 - Process coefficients for problem of interest (**Stage 3**)

9x9 array of assemblies in a pool



Rapid : Code System Structure



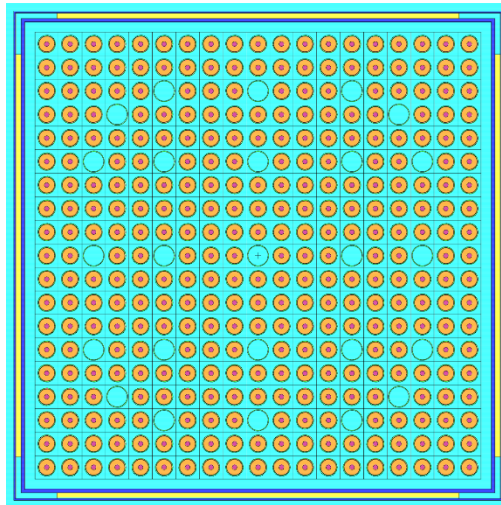
I²S-LWR –Reference Model

I²S-LWR FUEL ASSEMBLY

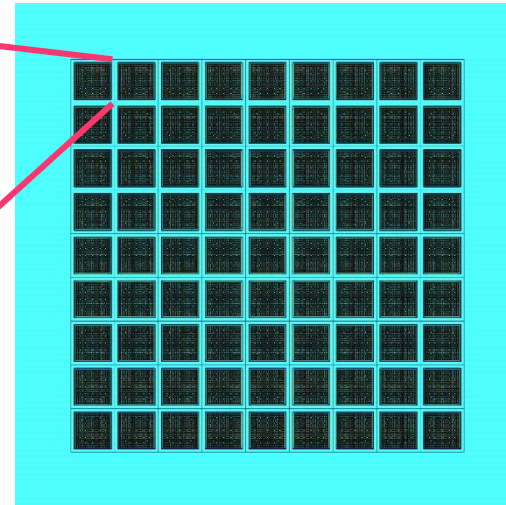
- 19x19 fuel lattice
 - 335 fuel rods, 24 control/guide tubes, 1 instrumentation tube
- U₃Si₂ fuel enriched to 4.95 wt-% ²³⁵U

SPENT FUEL POOL

- Based on AP1000 SFP
- Consider a 9x9 segment of SFP (81 assemblies)
- Storage cell walls made of Metamic® (B4C-Al) between SS plates



Assembly in a Storage Cell

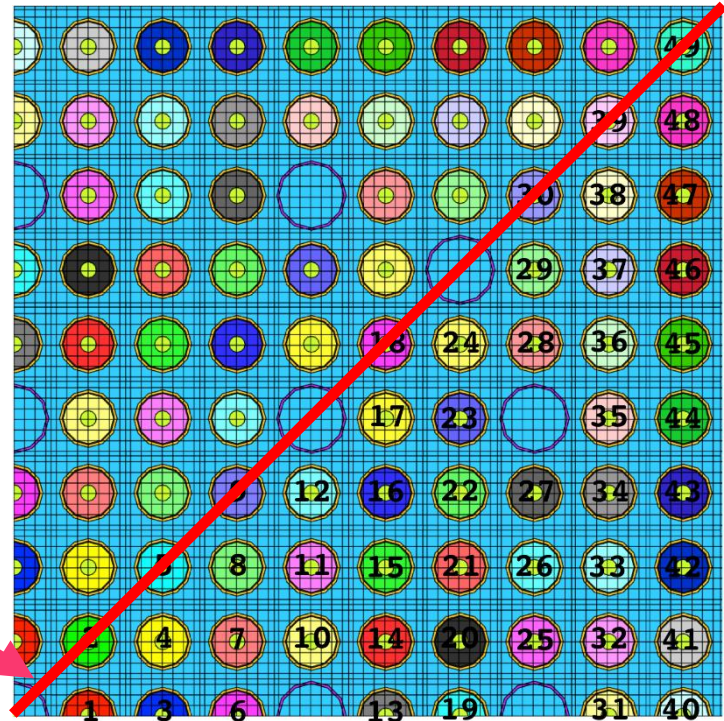


9x9 Segment of SFP

Pre-Calculation – p³RAPID

Stage 1: Burnup Calculation with SCALE/TRITON

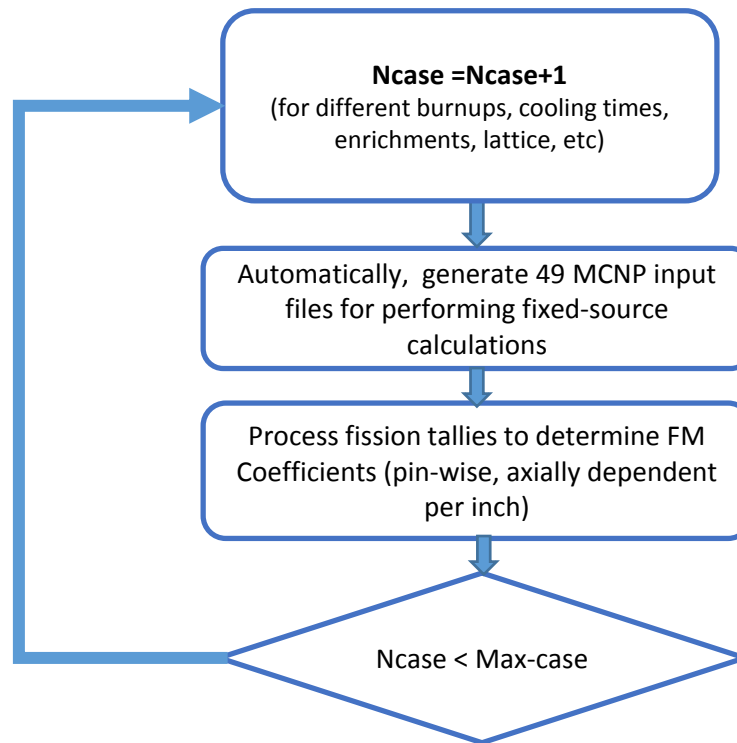
- **Need** : Material composition & Intrinsic source
- **Use**: SCALE 6.1 - TRITON
 - The TDEPL option used to invoke NEWT 2D & ORIGEN
- **For**:
 - enrichment of 4.95 wt-%; burnups: 37, 59 GWd/MTHM; and, Cooling Times: 14 days, 1 & 9 years
 - Quarter assembly model used.
 - 49 different fuel materials (considering octal symmetry)



Pre-Calculation – P³RAPID

Stage 2: Coefficient calculations

- Using information from Stage 1,



- A database of FM coefficient is prepared

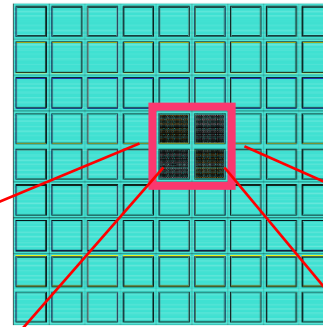
Comparison of RAPID with MCNP reference calculation

Test cases

- Performed eigenvalue calculations for a 2x2 segment of the reference SFP.
 - 4 test cases are defined, each containing different combinations of burnups/cooling times
 - Fuel region of the model partitioned into **32,256** fission regions (tallies)
- Reference MCNP eigenvalue parameters are:
 - 10^6 particles per cycle,
 - 400 skipped cycles
 - 400 active cycles

Description of Test cases – Pool segments

POOL



CASE 1

0 GWd/MTHM	37 GWd/MTHM
0 yr	0 yr
37 GWd/MTHM	0 GWd/MTHM
0 yr	0 yr

CASE 2

0 GWd/MTHM	59 GWd/MTHM
0 yr	0 yr
59 GWd/MTHM	0 GWd/MTHM
0 yr	0 yr

CASE 3

59 GWd/MTHM	37 GWd/MTHM
9 yr	0 yr
37 GWd/MTHM	59 GWd/MTHM
0 yr	9 yr

CASE 4

59 GWd/MTHM	37 GWd/MTHM
9 yr	9 yr
37 GWd/MTHM	59 GWd/MTHM
9 yr	9 yr

Burnup [GWd/MTHM]

Cooling Time [years*]

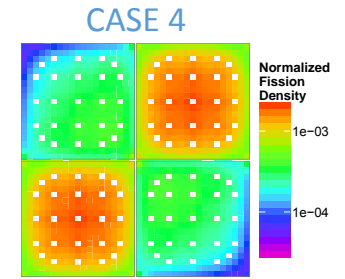
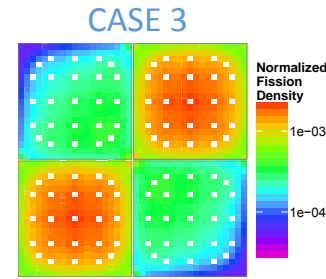
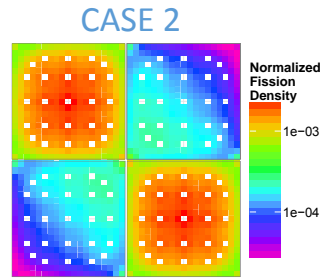
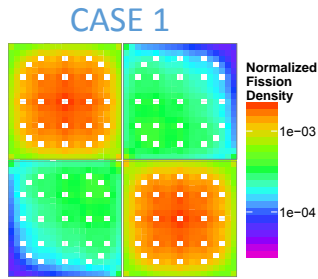
*'0 year' cooling time refers to ~14 days

Comparison of Eigenvalues

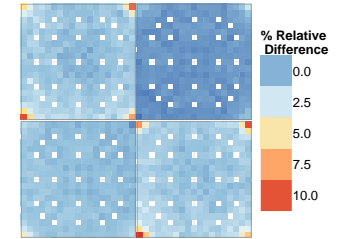
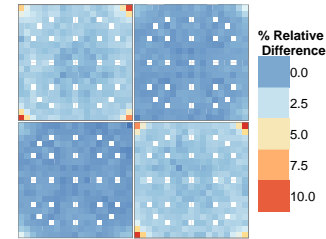
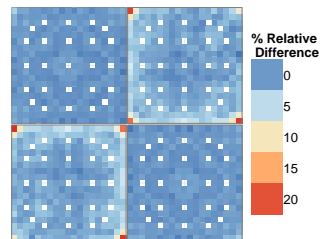
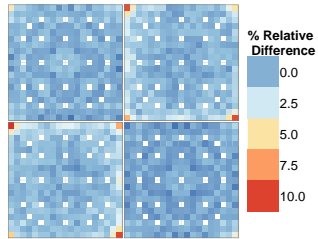
Case	MCNP	RAPID	Rel. Diff. RAPID vs. MCNP (pcm)
	k_{eff}	k_{eff}	
1	0.79998 (± 4 pcm)	0.80020	28
2	0.79511 (± 4 pcm)	0.79532	26
3	0.60444 (± 3 pcm)	0.60425	-31
4	0.58330 (± 3 pcm)	0.58322	-14

Comparison Radial fission densities (FD)

RAPID
Calculated Fission Densities



Relative Difference
w/ MCNP
Reference



Relative Difference
for assembly FD
totals

0.04%	0.68%
0.78%	-0.32%

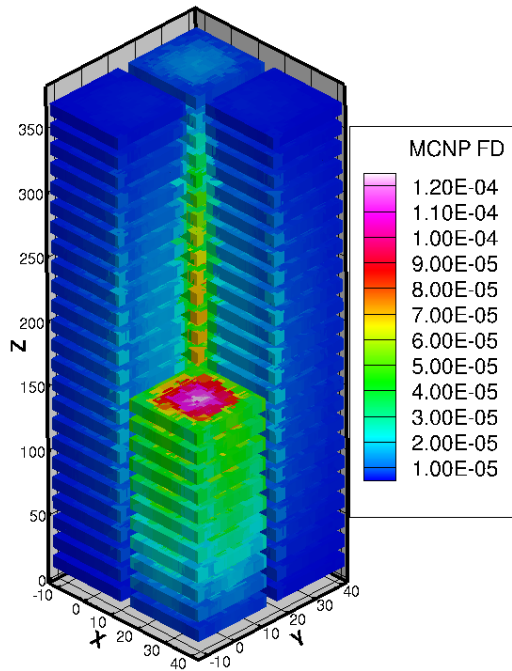
-0.27%	2.05%
2.09%	-0.15%

1.44%	-0.20%
-0.32%	1.45%

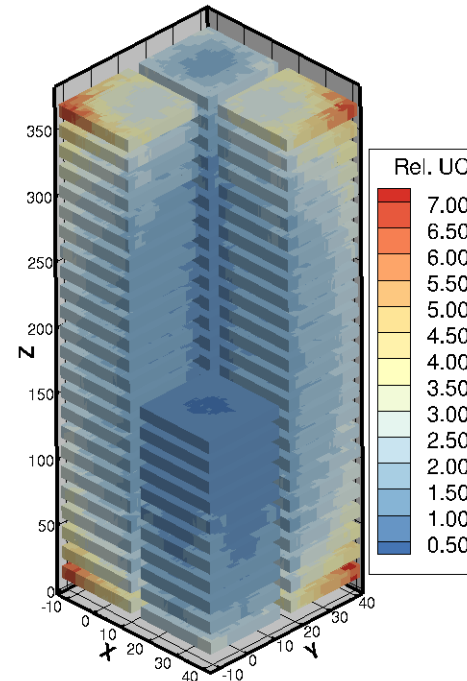
1.03%	-0.98%
0.53%	1.18%

MCNP Predictions (CASE 1)

Fission Density

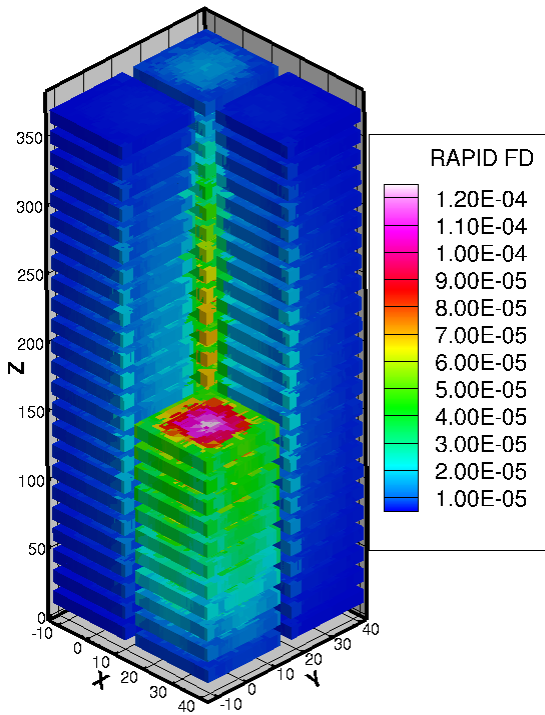


1- σ Relative Uncertainty

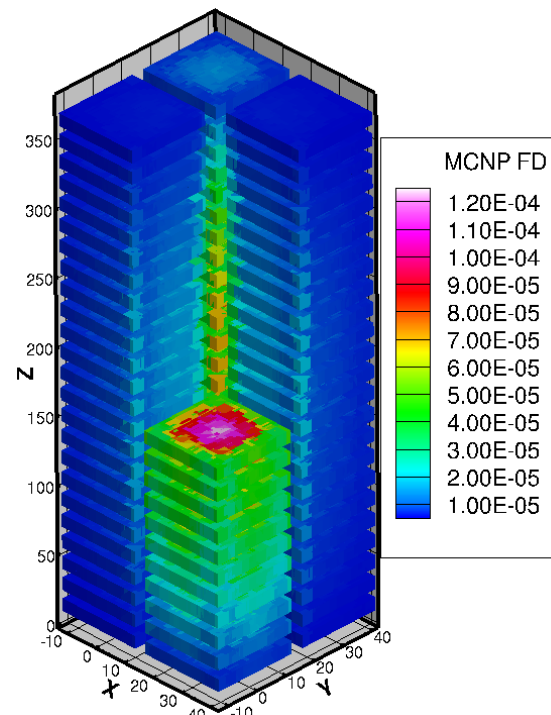


RAPID VERSUS MCNP(CASE 1)

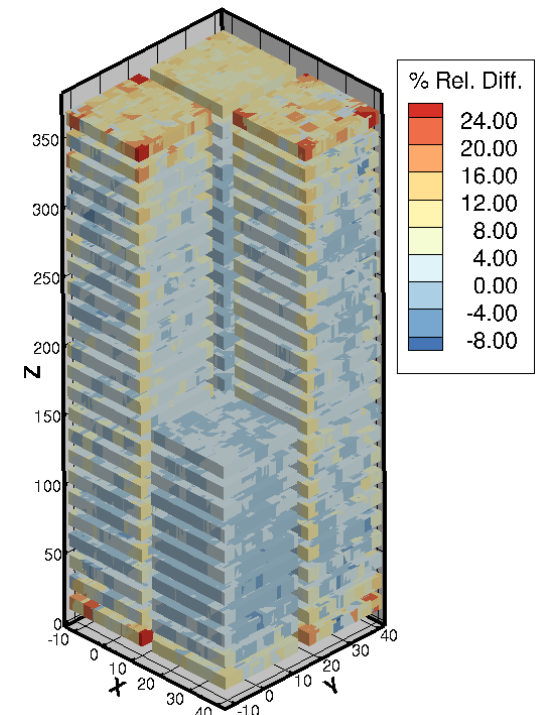
RAPID



MCNP

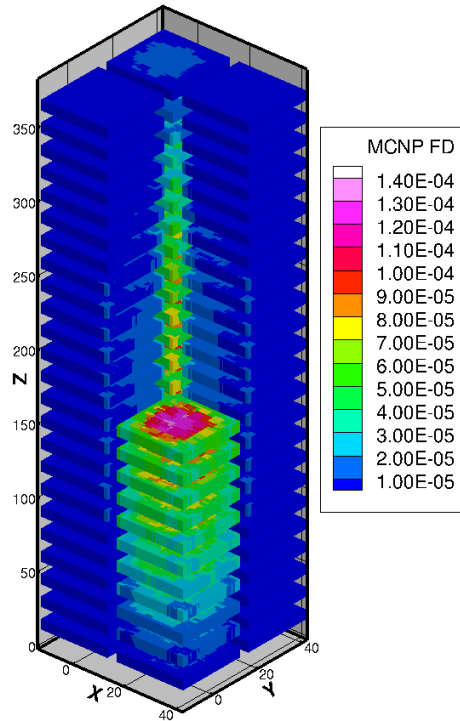


% Relative Difference

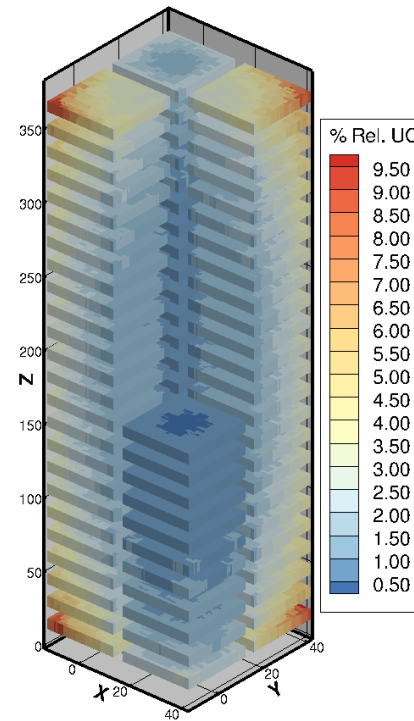


MCNP Predictions (CASE 2)

Fission Density

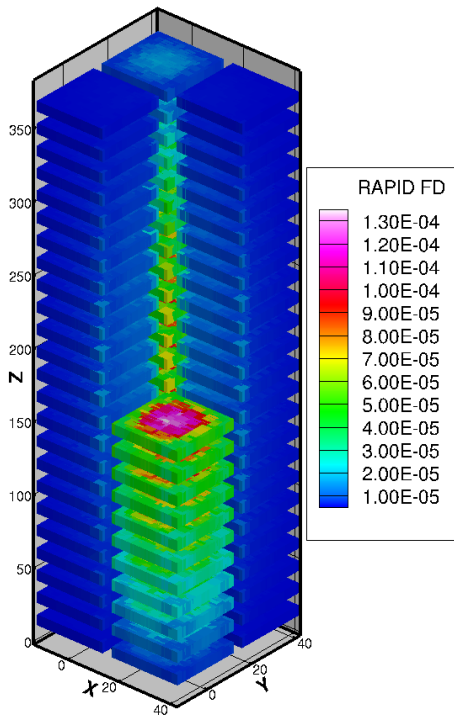


1- σ Relative Uncertainty

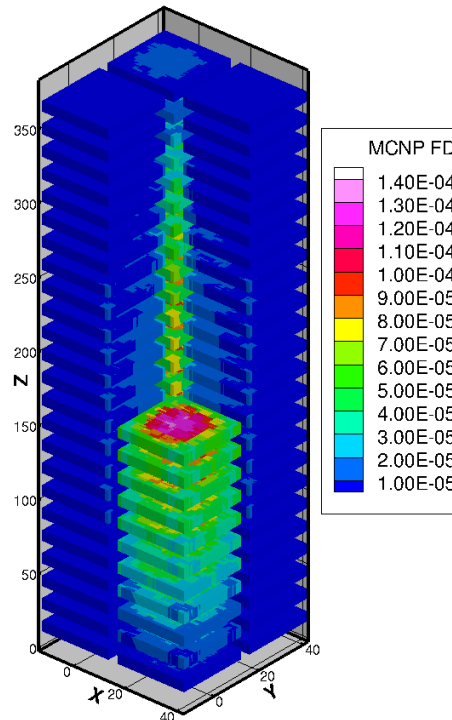


RAPID VERSUS MCNP (CASE 2)

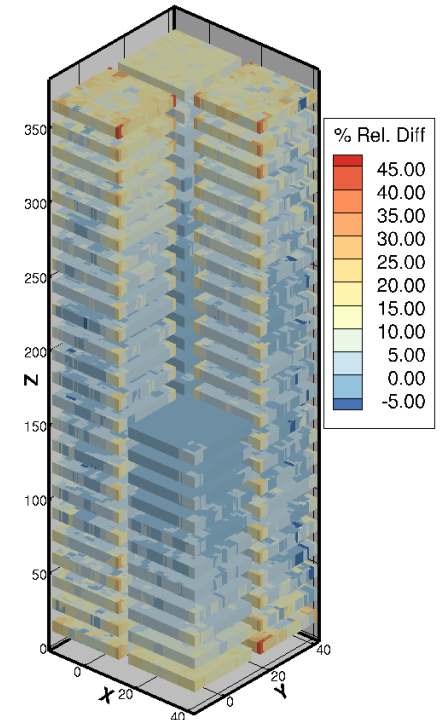
RAPID



MCNP

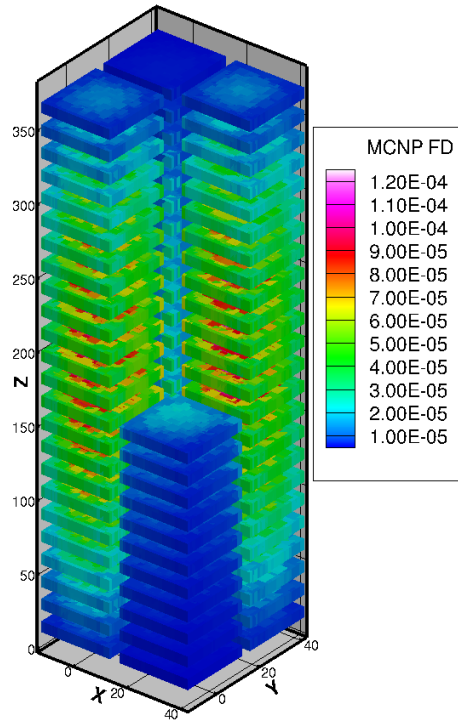


% Relative Difference

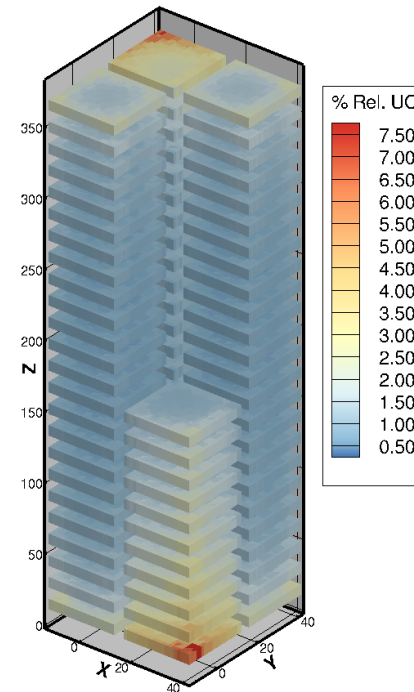


MCNP Predictions (CASE 3)

Fission Density

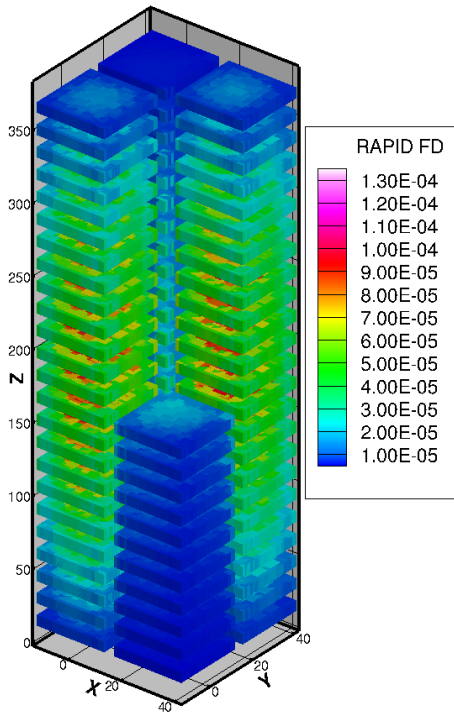


1- σ Relative Uncertainty

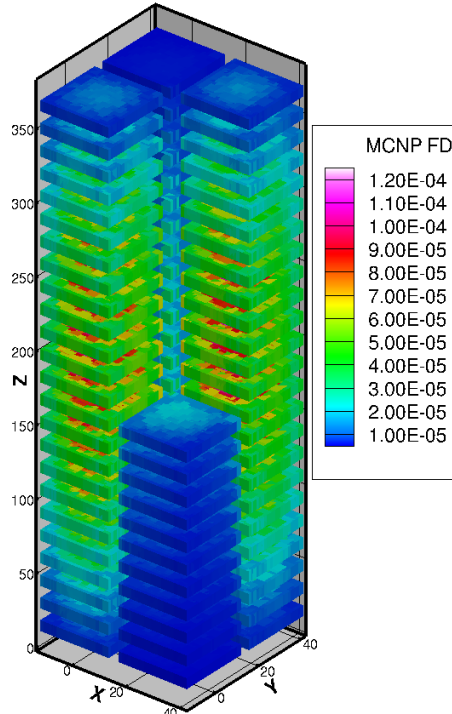


RAPID VERSUS MCNP (CASE 3)

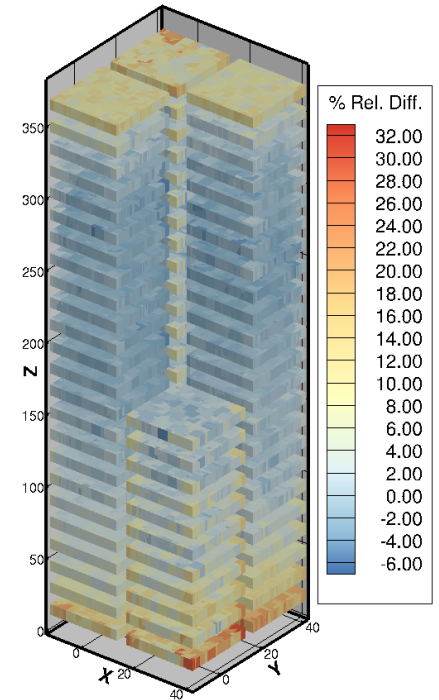
RAPID



MCNP

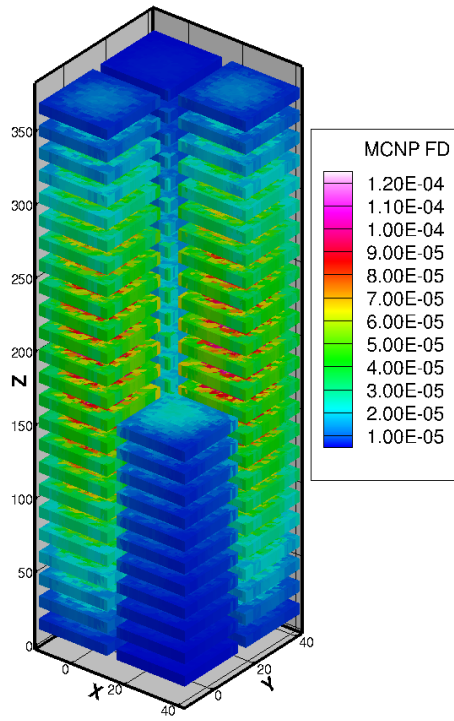


% Relative Difference

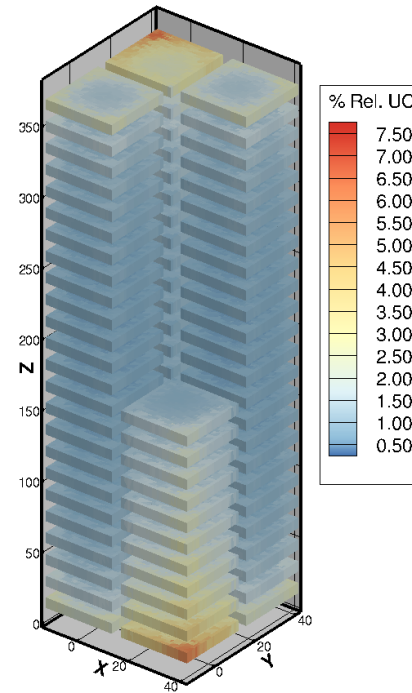


MCNP Predictions (CASE 4)

Fission Density

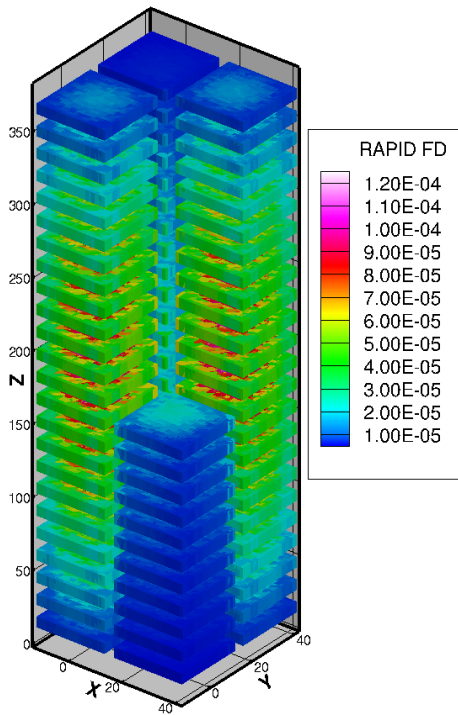


1- σ Relative Uncertainty

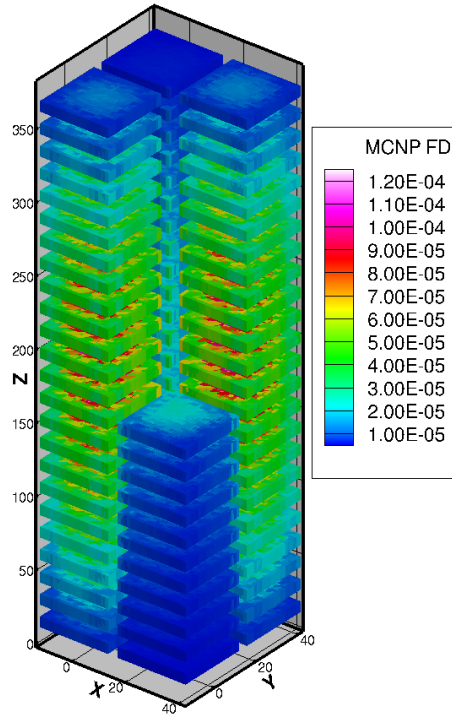


RAPID VERSUS MCNP (CASE 4)

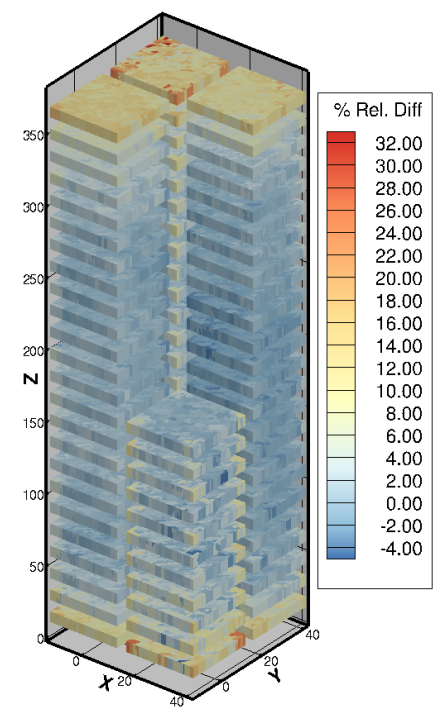
RAPID



MCNP



% Relative Difference



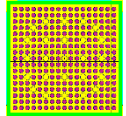
Computation Time

Case	MCNP		RAPID		
	Cores	Time [min)	Cores	Time [min]	Speedup
1	16	1020 (17 hrs)	1	0.50	2044
2	16	1013 (17 hrs)	1	0.51	1980
3	16	1082 (18 hrs)	1	0.50	2163
4	16	1149 (19 hrs)	1	0.50	2284

Comparison of RAPID to MCNP reference models

- Single assembly & full cask models -

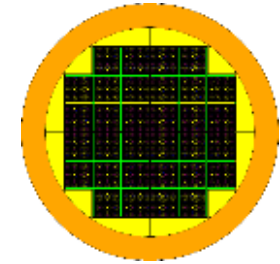
RAPID vs. MCNP – Single assembly model



- RAPID calculated and MCNP system eigenvalue (k_{eff}) and pin-wise, axially-dependent fission density distribution, i.e, **6,336 tallies**, are compared.
- **Significant speedup** is obtained using RAPID on just a single computer core.

Case	MCNP	RAPID
k_{eff}	1.18030 (± 2 pcm)	1.18092
k_{eff} relative difference	-	53 pcm
Fiss. density adjusted rel. uncertainty	0.48%	-
Fission density relative diff.	-	0.65%
Computer	16 cores	1 core
Time	666 min (11.1 hours)	0.1 min (6 seconds)
Speedup	-	6,666

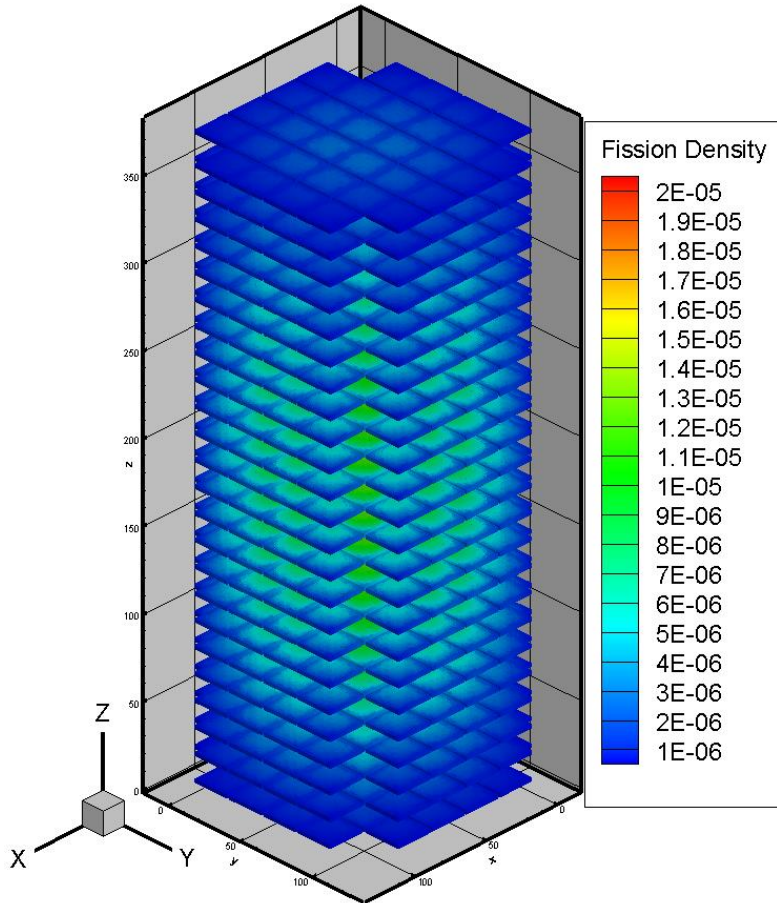
RAPID vs. MCNP – Full cask model



- RAPID calculated and MCNP system eigenvalue (k_{eff}) and pin-wise, axially-dependent fission density distribution, i.e, **202,752** tallies, are compared.
- **The speedup increases with the dimension of the model.**

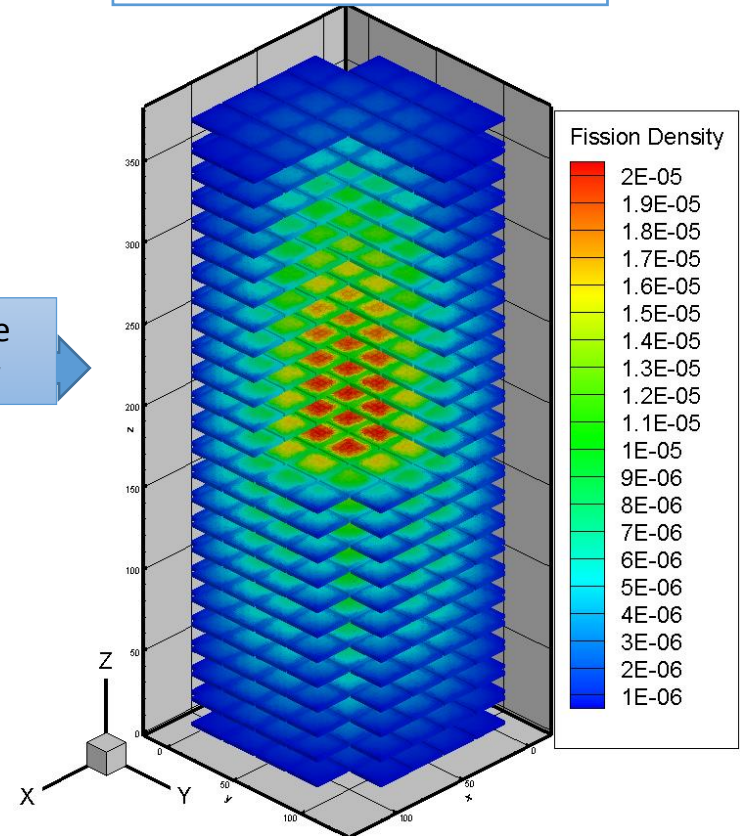
Case	MCNP	RAPID
k_{eff}	1.14545 (\pm 1 pcm)	1.14590
Relative Difference	-	39 pcm
Fission density rel. uncertainty	1.15%	-
Fission density relative diff.	-	1.56%
Computer	16 cores	1 core
Time	13,767 min (9.5 days)	0.585 min (35 seconds)
Speedup	-	23,533

GBC-32 3D fission density distribution



Inside view

With a quarter Blanked



Determination of neutron *Dose*



- Given the *neutron dose-to-flux ratio* (f_n) $\left(\frac{\frac{mrem}{hr}}{\frac{\#}{cm^2-s}}\right)$, then

$$Dose = \langle \psi f_n \rangle$$

- Then, Dose is calculated using the adjoint-function methodology by

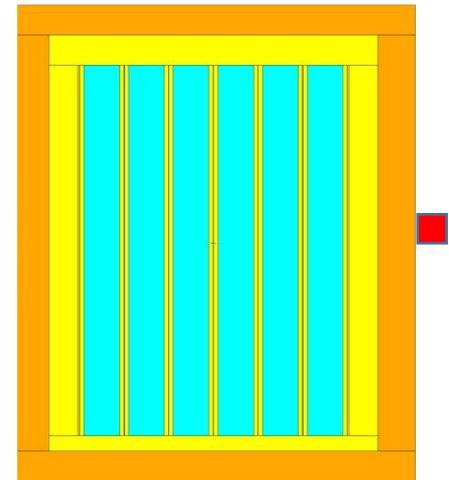
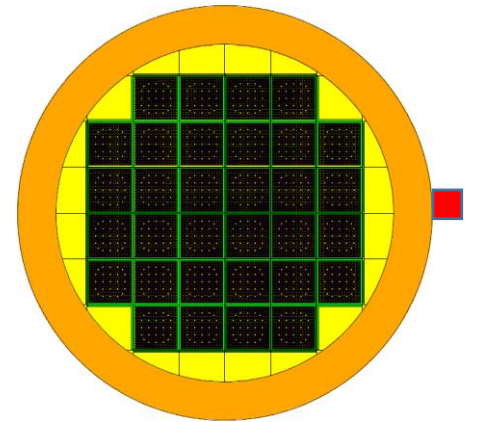
$$Dose = \langle \psi^* S \rangle$$

Where,

$$H^* \psi^* = f_n$$

TITAN Calculation Model

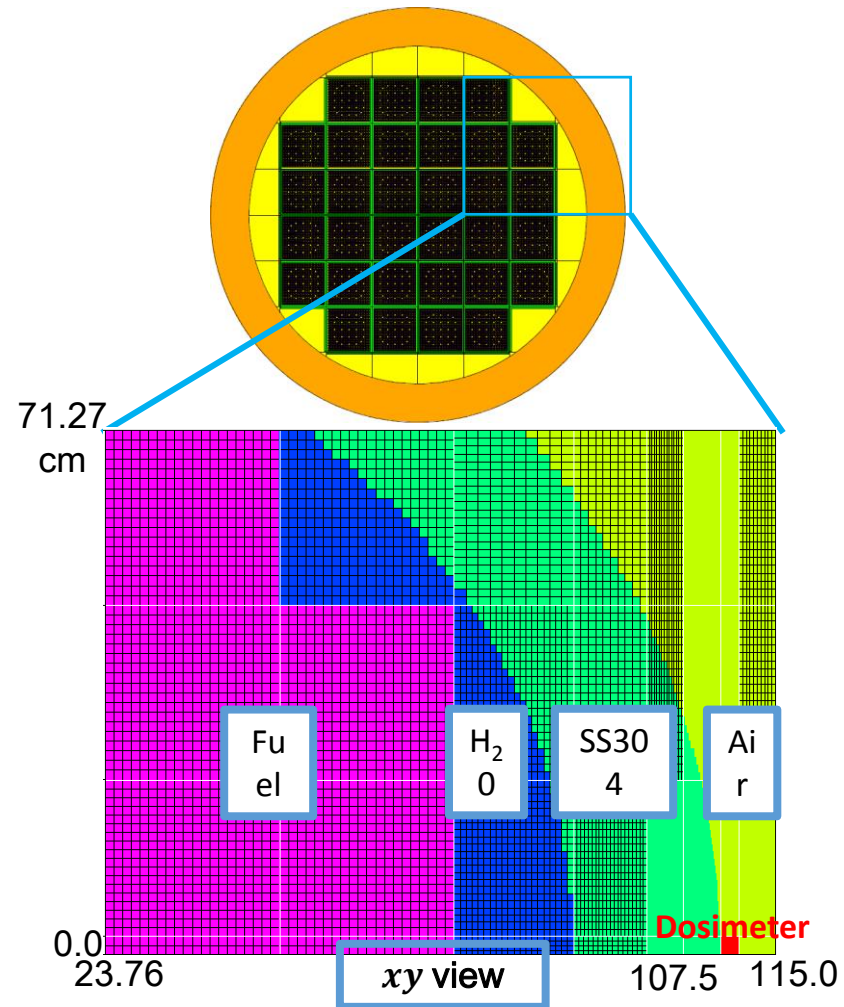
- Multigroup cross-section (energy group structure, Pn order)
- Calculation model (segment of the cask), Field-Of-View (FOV)?
- Spatial meshing, angular quadrature order, finite-differencing formulation, convergence



115.0

TITAN calculation

1. 2-assembly model
2. size = $91.24 \times 71.27 \times 40 \text{ cm}^3$
3. 2.5cm x 2.5cm x 5cm voxel
air detector
4. # meshes = 386,286,
5. S10 angular quadrature set
6. P3
5. 19-group [BUGLE-96 library;
groups 3-21]
6. 8 cores
7. 70 min



Dose calculation

- The dose formulation (i.e., detector response) is expressed by:

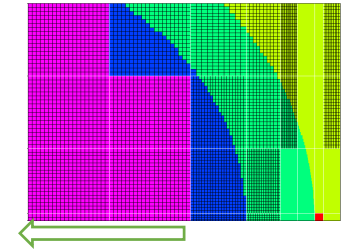
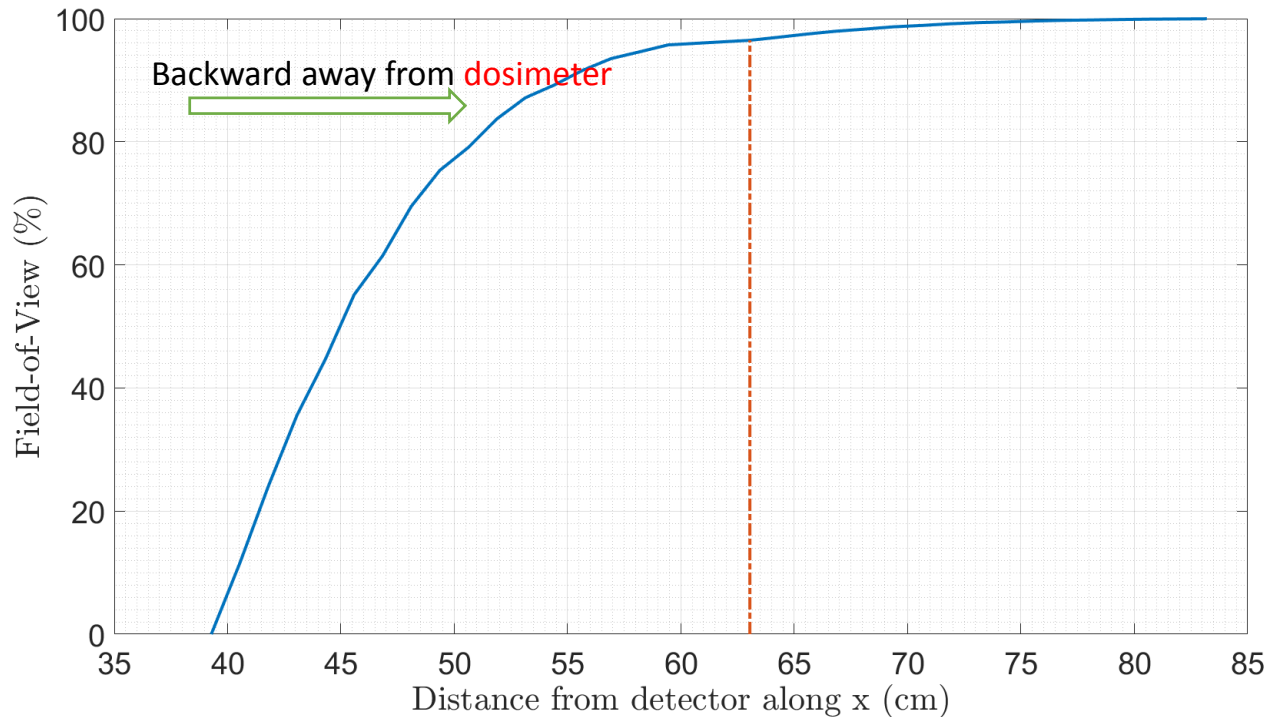
$$D = \sum_{g=3}^{21} \sum_{i=1}^{N_{cell}} \psi_{i,g}^* (\chi_g S_i)$$

χ_g is the *Watt spectrum* for energy group g , $\psi_{i,g}^*$ is the *importance function* of cell i for group g , and S_i is the RAPID calculated neutron source in cell i .

- The calculated dose is:

$$\text{Dose per unit source} = 7.79 \cdot 10^{-12} \left[\frac{\text{rem}}{\text{hr}} \right]$$

Detector field-of-view



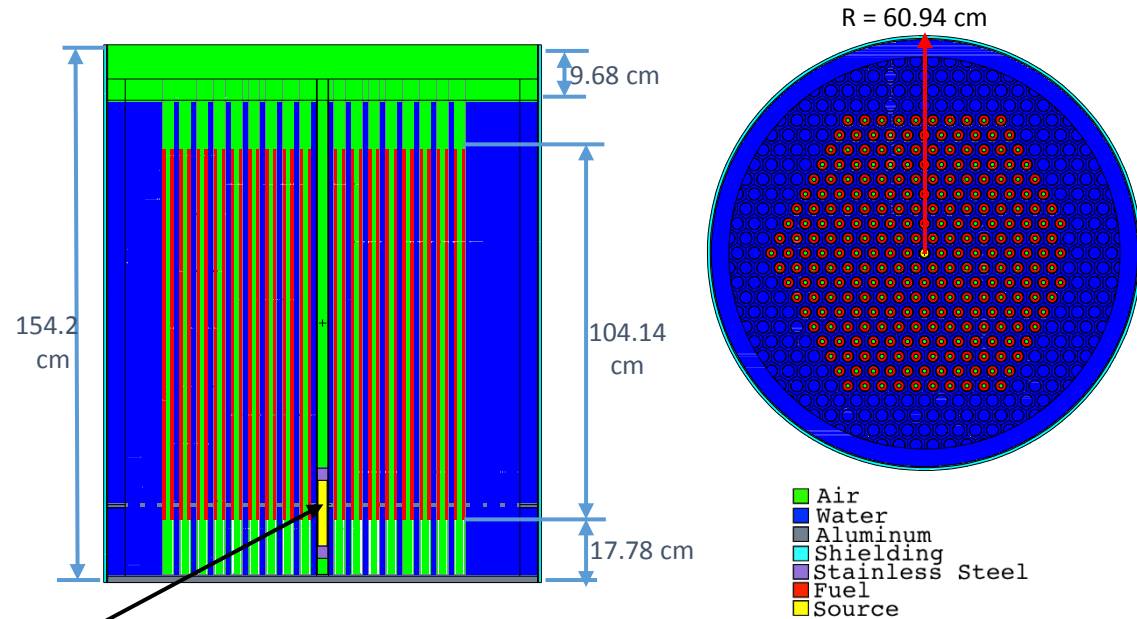
- **More than 90% of the dose evaluated at the canister's surface is due to the outermost row of assemblies, near the boundary.**

Experimental Benchmarking of RAPID

Phase 1

Benchmark facility - US Naval academy Subcritical (USNA-SC)

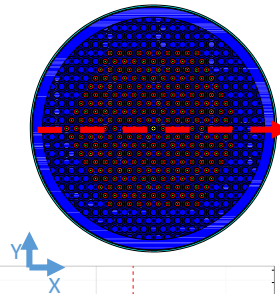
- A cylindrical pool with natural uranium (fuel) and light water (moderator)
- There are a total of 268 fuel rods, arranged in a hexagonal lattice
- Fuel: hollow aluminum tubes containing 5 annular fuel slugs
- Neutron source: PuBe



Whole Core - Total Neutron Flux

Cross Core Slice
($y=0\text{cm}$ & $z=-102\text{cm}$)

Source
Centerline



Axial Profile
($x=0$ & $y=0$)

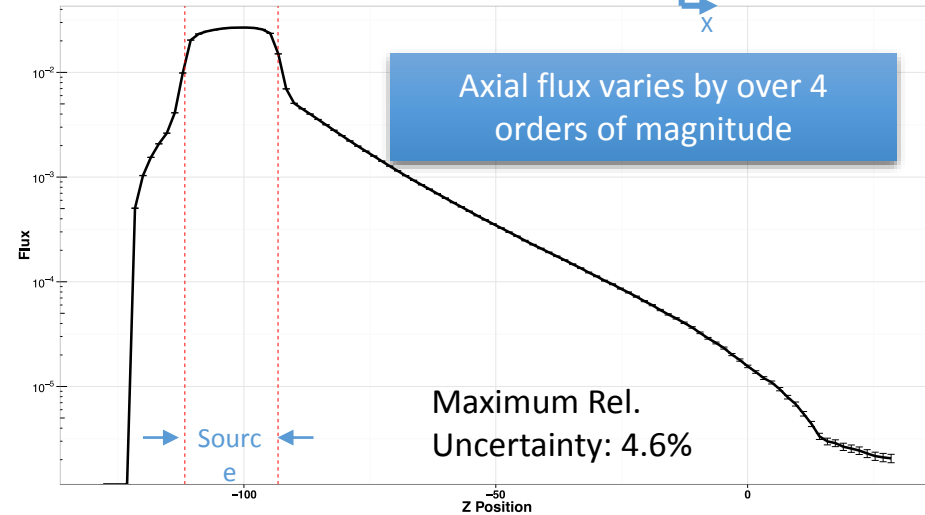


Maximum Rel.
Uncertainty: 4.8%

Radial flux drops by 4 orders of magnitude

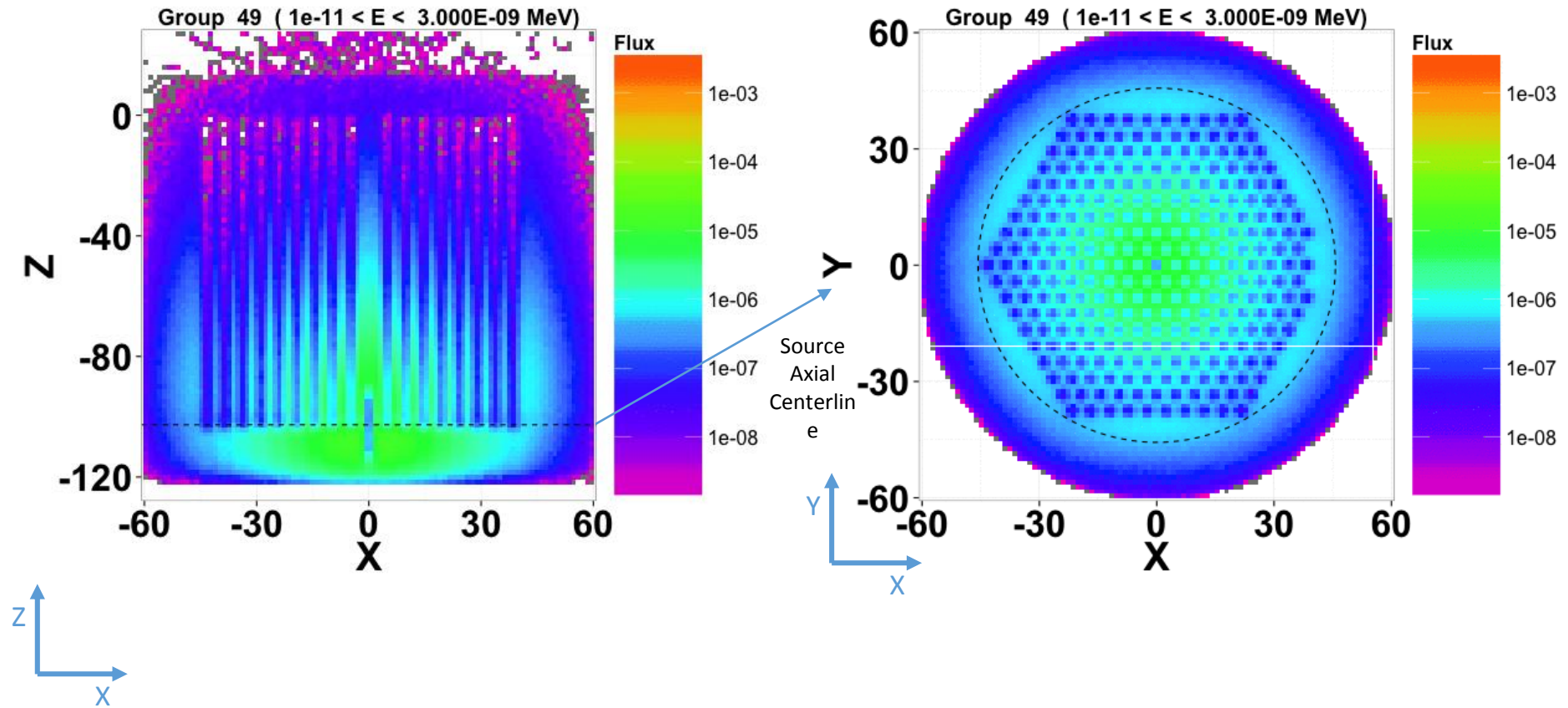
Active Fuel Region

Y Position

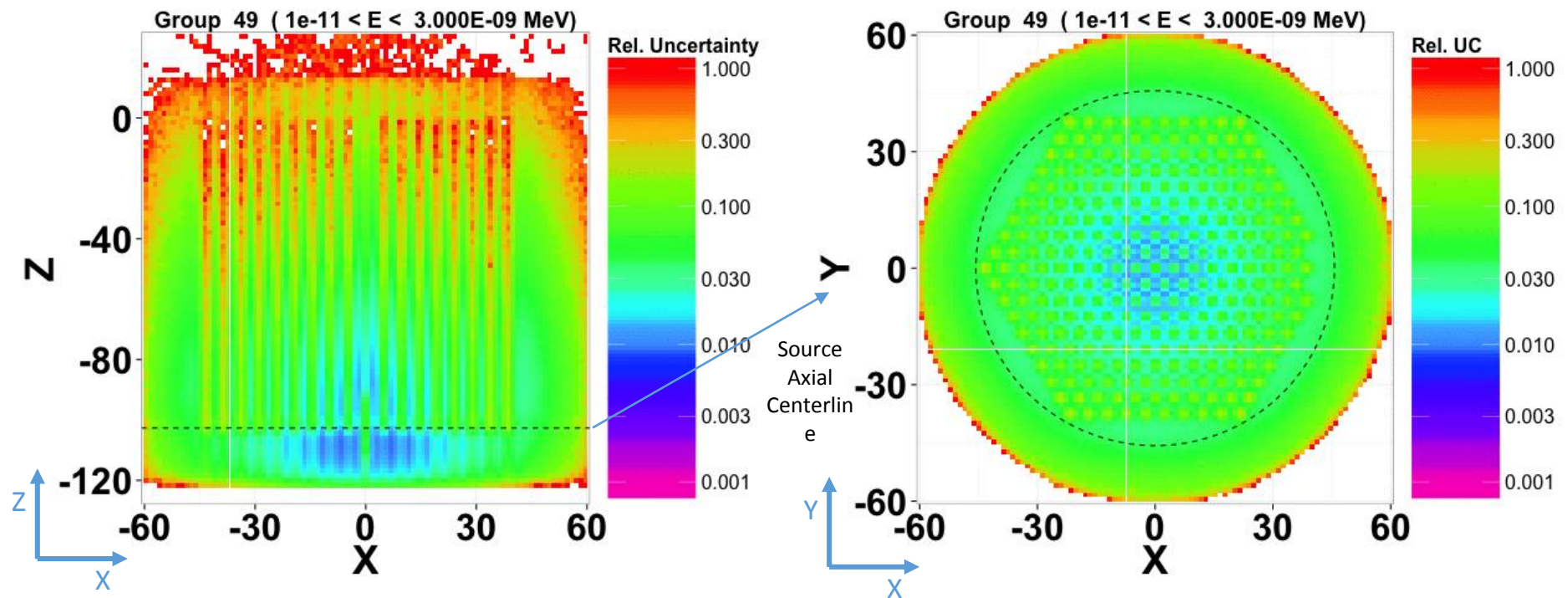


Maximum Rel.
Uncertainty: 4.6%

Whole Core : Neutron flux Distribution

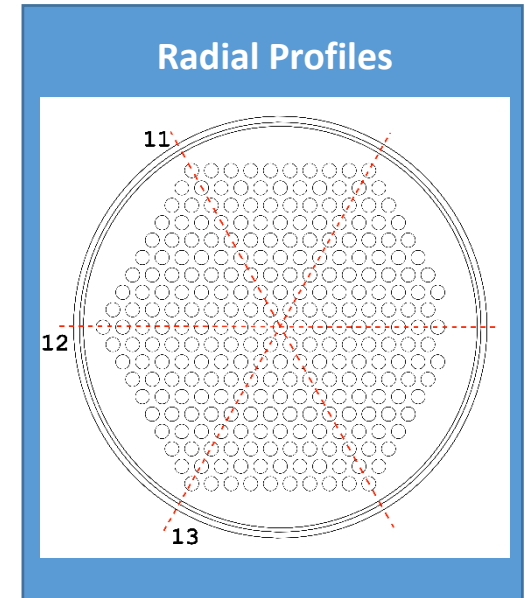
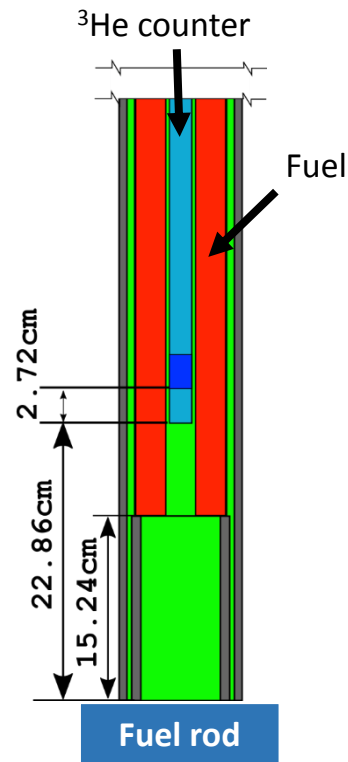


Whole Core : Relative Uncertainties of Neutron Flux



Experiments

- Count rate in a ^3He proportional counter was measured by placing the counter within the annulus of each fuel pin
- Neutron counts are determined in fuel pins along three radial profiles (11, 12, & 13) shown in the figure.



Comparison of reaction rates (Counts) of ^3He detector

[experiment vs calculation]

estimated Detector Efficiency based on least-squares minimization

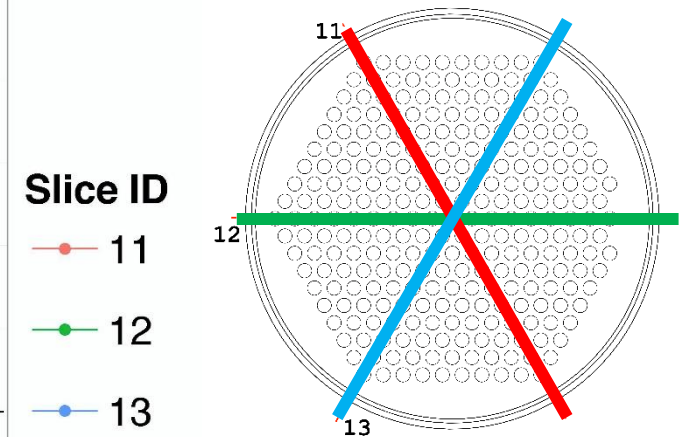
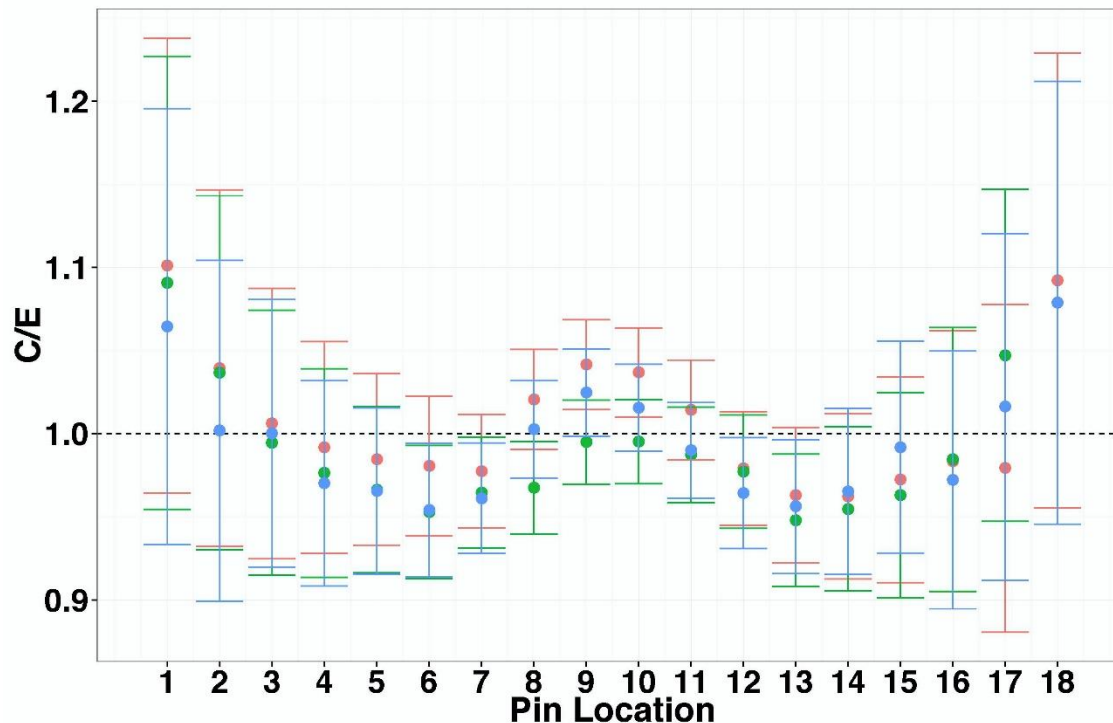
$$Eff = \frac{\sum_i c_i m_i}{\sum_i c_i^2}$$

Where,

m_i = Measured response at position i

c_i = Calculated response at position i

$f = \frac{c}{m}$ (Ratio of calculated to measured responses)



Estimation of uncertainty in $f = \frac{c}{m}$

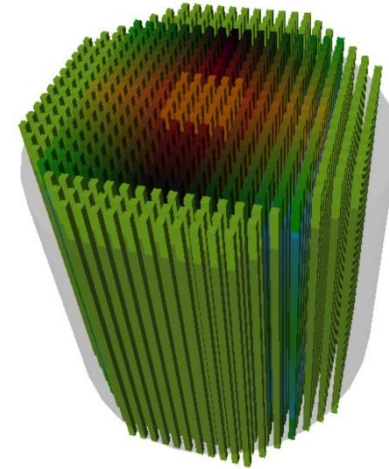
$$= \sqrt{\frac{\sigma_c^2}{m^2} + \frac{c^2 \sigma_m^2}{m^4}}$$

Virtual Reality - Phase 1

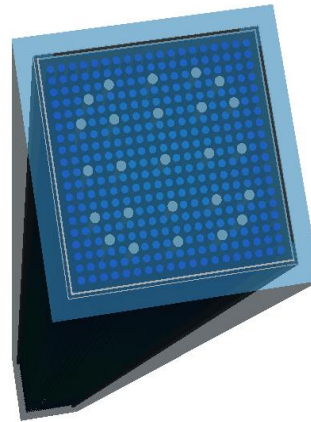
- Two of my graduate students (*Nate Roskoff and Val Maslcolino*) are working with me and *Drs. Polys and Rajamohan* and a student from School of Arts and Design in this project
- Tasks
 - Development of a **connectivity environment** between the visualization systems in *Blacksburg and Arlington*. This will make possible seamless interaction in a virtual environment between collaborators that are geographically separated.
 - Development of a **VRS for a spent nuclear fuel pool**. This virtual model tool includes our RAPID code system for monitoring the pool in real time.
- We have developed software using *Paraview* and *x3dom* packages (examples are available at <http://nrel.ncr.vt.edu/vrs.html>)

Examples

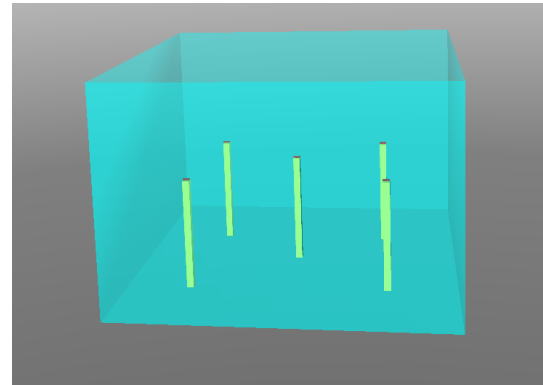
- [Prototype S3NPower](#)



- [Typical PWR Fuel Assembly](#)



- [Virtual Spent Fuel Pool](#), [Virtual pool-assembly](#) & real-time RAPID calculation



Conclusions

- MRT methodology allows for development of real-time tools for analysis of nuclear systems
- Thus far, we have developed
 - INSPCT-S, AIMS, TITAN-IR, & RAPID
- We have demonstrated that indeed we obtain accurate, detailed solution in real time!
- This is especially true for RAPID code system that has been applied to the simulation of spent fuel pools and casks
 - Pin-wise, axially dependent fission density is determined in 35 seconds
- Further, it is demonstrated that after about 18 hours of calculation MCNP has not fully convergence near the absorber racks, i.e., difficulties with undersampling.
 - *Standard eigenvalue Monte Carlo has difficulties with HDR, undersampling, and correlation*
 - *The FM approach used in RAPID is a solution to above difficulties*
 - The RAPID MRT algorithm is able to **overcome the main issues** related to Monte Carlo eigenvalue calculations such as source convergence and cycle-to-cycle correlation

Ongoing & Future Studies

- Continued sensitivity analysis of RAPID for different burnups
- Complete experimental benchmarking of RAPID using the U.S. Naval Academy's subcritical facility
 - Preliminary experimental benchmarking results were presented at the recent INMM meeting, July 2016.
- Initiated determination of statistical uncertainties associated RAPID calculated eigenvalue and fission density
 - i.e., Propagation of the uncertainties of the FM coefficients
- External dose/detector response calculation has been implemented in RAPID using the TITAN-calculated importance function methodology*
- Extend RAPID for material identification
- An automated methodology for the determination of the FOV of a detector is under development.
- TITAN dose calculation will be benchmarked against a reference A³MCNP (Automated Adjoint Accelerated MCNP) code prediction.
- Developing virtual reality system for a spent fuel pool

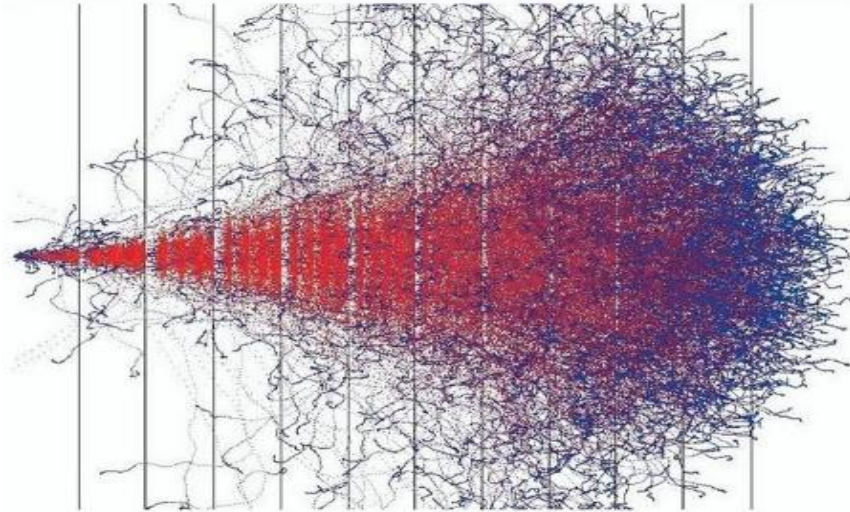
Thanks!

Questions?



A new book

Monte Carlo Methods for Particle Transport



Alireza Haghghat

 CRC Press
Taylor & Francis Group